Plant Stress 16 (2025) 100855

Contents lists available at ScienceDirect

Plant Stress

journal homepage: www.sciencedirect.com/journal/plant-stress

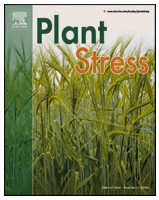

"Sensing, learning but forgetting": the inability of strawberry plants to transmit the infochemically-mediated stress priming under salinity

Costanza Ceccanti [a,1], Giulia Lauria [a,1], Fabrizio Araniti [b], Ermes Lo Piccolo [c], Ylenia Pieracci [d], Guido Flamini [d], Lucia Guidi [a], Marco Landi [a,*]

[a] Department of Agriculture, Food and Environment, University of Pisa, Pisa, Italy
[b] Department of Agricultural and Environmental Sciences - Production, Landscape, Agroenergy, University of Milan, Milan, Italy
[c] Department of Agriculture, Food, Environment and Forestry, University of Florence, Florence, Italy
[d] Department of Pharmacy, University of Pisa, Pisa, Italy

ARTICLE INFO

Keywords:
Plant-plant communication
Primary metabolism
Salt stress
Volatilome
Abiotic stress

ABSTRACT

Volatile Organic Compounds (VOCs) are widely recognized for their role in priming neighbouring plants against pathogens and herbivores, whilst their involvement in airborne-mediated priming under abiotic stress remains largely unexplored. With a 3-step experiment, we tested the hypothesis that VOC emissions by salt-stressed plants can prime neighbouring conspecific individuals once subjected to salinity. In step 1, salt-stressed (60 mM NaCl for 20 days; emitters – *C*+NaCl) strawberry plants (*Fragaria* × *ananassa* var. Elsanta) were grown together with receiver individuals irrigated with water only (NaCl-*S*). In step 2, a subset of NaCl-*S* plants was exposed to salt stress (NaCl-*S*+NaCl), while others were co-grown in a plastic box with additional unstressed strawberry plants (super receiver - NaCl-*SS*). Lastly, in step 3, NaCl-SS plants were treated with salt stress (NaCl-SS+NaCl). Control (C) – irrigated with water only – and *C*+NaCl plants of the same age as treated plants, were maintained as references for each step. In step 2, no differences were detected in terms of biomass, gas exchange parameters and chlorophyll content in NaCl-*S*+NaCl compared to non-stressed plants, thus confirming an enhanced stress tolerance mediated by infochemicals from emitters. Furthermore, in step 3, NaCl-SS+NaCl mirrored the performances of emitters, suggesting that no efficient airborne signal transmission took place from NaCl-S to NaCl-SS. The dataset offers evidence that neighbouring plants can perceive airborne signals, altering their metabolic profile and enhancing stress tolerance when subsequently stressed. Moreover, we demonstrate that, despite being primed, receivers cannot propagate the signal to their neighbouring conspecific individuals.

1. Introduction

Plant-plant interaction, a topic introduced by Cleave Backster in the 1960s and accepted with skepticism by the scientific community at that time (Backster 2003), is in continuous evolution. The discovery of "communication" mediated by volatile organic compounds (VOCs) marked a turning point in the comprehension of inter-plant communication through the perception of airborne signals (Baldwin and Schultz 1983).

Although knowledge about plant-environment interactions mediated by VOCs, including plant-to-plant communication, remains limited, growing evidence supports the benefits of in-planta VOC-mediated signaling (Heil and Karban, 2010, reviewed by Karban, 2015). In particular, sessility implies that plants have evolved an arsenal of molecular compounds to sense, perceive, respond, and adapt to external stimuli (Baluška 2009). These mechanisms can occur either actively or passively (Li and Blande 2015). The active mechanism includes a response by the receiver plant, exposed to emitter VOCs, which can be commonly observed at biochemical or physiological levels (e.g., changes in plasma transmembrane potential, production of superoxide anion and H_2O_2, jasmonic acid or salicylic acid level promotion, up-regulation of lipoxygenase gene – for a review see Brosset and Blande 2022). On the other hand, a passive mechanism involves the adsorption of volatiles emitted by neighbouring plants (e.g., the sequestration by cuticular waxes or adhesion of VOCs to the surface of a receiver plant) and their passive re-emission in the environment. This indirect pathway of

* Corresponding author.
E-mail address: marco.landi@unipi.it (M. Landi).
[1] The authors contributed equally.

https://doi.org/10.1016/j.stress.2025.100855
Received 11 February 2025; Received in revised form 18 March 2025; Accepted 11 April 2025
Available online 17 April 2025

VOC-mediated interactions remains an underexplored yet potentially significant aspect of plant communication (Himanen et al., 2010; Camacho-Coronel et al. 2020). Both mechanisms can lead to alterations in the VOCs emitted by receiver plants, either as an immediate reaction, a consequence of abiotic stress-induced changes, or a primed response to stress.

Typically, research on plant-plant interactions has focused on defense-related responses, as VOCs released by herbivore- or pathogen-damaged plants serves as cues of a potential attack, enabling neighboring plants to mitigate damage (Frost et al. 2008). Indeed, it has been observed that emitted VOCs, "eavesdropped" by neighbouring plants, conferring ecological and physiological advantages by priming them for herbivores or pathogen attacks (as reviewed by Yuan et al. 2009).

Besides biotic stressors, also environmental factors have a crucial impact on volatiles release from the plant (reviewed by Holopainen and Gershenzon, 2010 and by Landi et al., 2020). High temperature, high light intensities (Loreto et al., 2006), light qualities (Lauria et al., 2023), water stress, salt stress (Landi et al., 2020; Ciriello et al., 2023), metal toxicity (Bibbiani et al., 2018) have also been reported to increase VOC emissions in a wide range of plant species. In the case of salt stress, for example, a few experiments on basil plants reported an increased content in linalool and β-*cis*-ocimene (Ciriello et al., 2023) and bornil acetate and eugenol (Landi et al., 2020) in VOC composition, after the application of similar NaCl concentrations.

Despite the awareness that those VOC cues emitted by plants can be altered, little information is available on plant-plant interactions driven by abiotic stressors.

Recent studies suggest the presence of biochemical and physiological mechanisms developed by receiver plants involved in offsetting the costs associated with activating defense responses. (Engelberth and Engelberth, 2019). It has been shown that VOCs emitted by plants experiencing salt stress (emitters) can induce priming effect in nearby unstressed plants (receivers), increasing their resilience to salt stress. This phenomenon has been observed in Arabidopsis (Lee and Seo 2014), broad bean (*Vicia faba* L.; Caparrotta et al. 2018), and sweet basil (*Ocimum basilicum* L.; Landi et al. 2020) plants. Indeed, receivers could increase their photosynthetic efficiency or stomatal conductance (to sequestrate more CO_2) or promote root elongation (to absorb more nutrients). Despite Caparrotta et al. (2018) observed a substantial decrease in stomatal conductance and photosynthetic rate in receiver plants, in the second phase of the experiment, those previously primed for salt stress and subsequently treated with 150 mM NaCl showed higher stomatal conductance, photosynthetic rate and relative growth rate compared to unprimed plants (non-eavesdropped plants in the first part of the experiment). On the contrary, Landi et al. (2020) reported no changes in photosynthetic efficiency upon receipt of a volatile cue and, in the second step of the experiment, receivers subjected to salt stress exhibited a more drastic decrease in photosynthesis compared to controls. However, in this species, the airborne signals emitted by salt-stressed plants promoted earlier flowering and a more abundant seed production in receivers, a strategy based on limiting damages by ensuring reproduction (Lucas-Barbosa et al. 2013).

As far as we are aware, only one study has been conducted to test whether receivers can "propagate" (actively and/or passively) the airborne signals triggered by VOC emitters subjected to salt stress (Falik et al. 2011). To address this knowledge gap, the present work aimed to highlight the physiological and biochemical changes between VOC-primed and unprimed plants in salt stress conditions. A three-step experiment was therefore designed to answer the following questions: i) does (and how) salinity affect salt-stressed strawberry plant metabolism and their volatilome?; ii) are salt-stressed strawberry plants (VOC emitters) able to prime neighbouring plants (VOC receivers) to have faster and more efficient defense responses when exposed to salt stress?; iii) are unstressed receivers able to propagate the message to neighbouring strawberry plants?

2. Materials and methods

2.1. Plant material and growing conditions

Experiments were conducted in a greenhouse at the Department of Agriculture, Food and Environment of the University of Pisa (43° 43′ 00″ N 10° 24′ 00″ E), Pisa, Italy. Cold-stored strawberry plantlets (*Fragaria* × *ananassa* var. Elsanta) were purchased from COVIRO s.r.l. (Cervia, RA, Italy) and transplanted into 1-L pots filled with a peat and perlite substrate (70:30; v/v). Plants were kept well-watered until the beginning of the experiment, and flowers and runners were removed periodically. Salt treatments started 20 days after the transplant, and the trial was organized into three steps. Each plant received 50 mL pot^{-1} day^{-1} of tap water, and salt treatment was administered by dissolving NaCl in the daily irrigation at a concentration of 60 mM (validated in a preliminary study performed by the authors; data not shown). Inside the greenhouse, the average air temperature, air relative humidity, and photosynthetically active radiation were ~25 °C, ~80 %, and ~600 μmol m^{-2} s^{-1}, respectively. During the three-step experiment, plants were kept in 0.6 m^3 plastic boxes to prevent communication between plants exposed to different treatments. The bottom of every box was absent to maintain balanced evapotranspiration, and pots were raised on a smash support, 100 cm above the floor.

2.2. Experimental design

The experiment was organized into three subsequent steps (Fig. 1), each lasting 20 days.

In each step, all plants were the same age. In step 1, the four boxes were filled with 20 plants, divided as follows: two boxes each contained 10 strawberry plants irrigated with the NaCl solution (emitters; $C{+}NaCl_{(20)}$) together with 10 plants irrigated with tap water (receivers; $NaCl\text{-}S_{(20)}$) in two separate rows. Two other boxes contained 20 control plants irrigated with tap water ($C_{(20)}$).

In step 2, the four boxes were filled with 12 plants as follows. In the first one, 6 $C_{(20)}$ plants were irrigated with the NaCl solution ($C{+}NaCl_{(40)}$), and 6 $C_{(20)}$ plants were irrigated with tap water. In the second box, to assess receiver responses to salinity, 6 $NaCl\text{-}S_{(20)}$ plants (receivers in step 1) were irrigated with the NaCl solution ($NaCl\text{-}S{+}NaCl_{(40)}$) and 6 $C_{(20)}$ plants were irrigated with tap water. In these two boxes, the plants irrigated with tap water were used to maintain constant evapotranspiration in the plastic containers, and they were not used for the analysis. In the third box 12 $C_{(20)}$ plants were irrigated with tap water, representing control plants ($C_{(40)}$). Finally, to investigate if a receiver could then behave as an emitter, 6 $NaCl\text{-}S_{(20)}$ plants (receivers in step 1) and 6 $C_{(20)}$ plants were placed in the last box, both irrigated with tap water and named $NaCl\text{-}S_{(40)}$ (emitters in step 2) and $NaCl\text{-}SS_{(40)}$ (receivers in step 2), respectively.

In step 3, to establish the physiological and biochemical behaviour of step 2 receivers under salt stress, only three boxes were maintained, each containing three plants. The first box contained 3 $NaCl\text{-}SS_{(40)}$ plants (receivers in step 2) irrigated with the NaCl solution ($NaCl\text{-}SS{+}NaCl_{(60)}$). The second box contained 3 $C_{(40)}$ plants irrigated with the NaCl solution ($C{+}NaCl_{(60)}$). Finally, the third box contained 3 $C_{(40)}$ plants irrigated with tap water, representing control plants of step 3 ($C_{(60)}$).

In all steps, leaf contact was avoided throughout the entire duration of the complete experiment.

2.3. Biomass, Na^+ and Cl^- content determination

The leaves of the plants from each step of the experiment were separated, their total biomass for each plant was recorded, and then an amount of them was sampled in liquid nitrogen until the biochemical analysis. To determine the dry matter percentage, another amount of the leaves was dried in a ventilated oven (Memmert GmbH Co. KG Universal

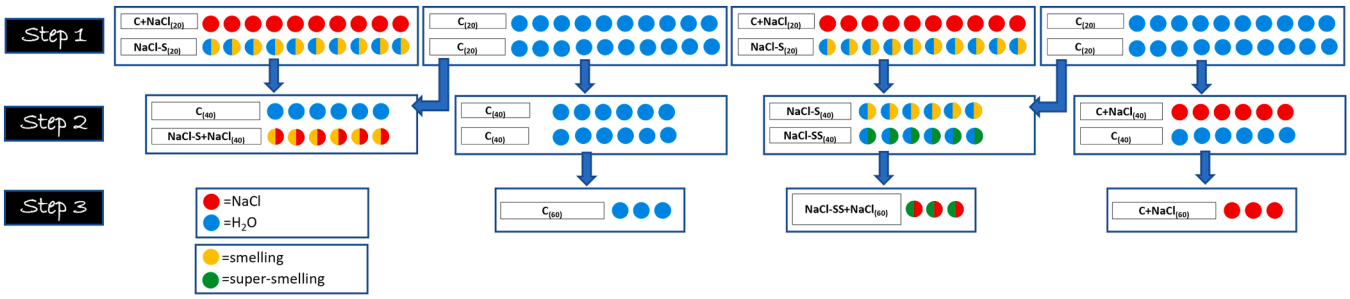

Fig. 1. The experimental design employed to test plant-plant communication. Step 1: $C_{(20)}$ represents control plants, $C+NaCl_{(20)}$ represents the plants treated with 60 mM NaCl for 20 days and NaCl-S represents the control plants exposed for 20 days to airborne cue emitted by $C+NaCl_{(20)}$ plants. Step 2: after 20 days, NaCl-S plants were treated with 60 mM NaCl, similar to control plants of the same age, which were not previously exposed to airborne cue, namely $C+NaCl_{(40)}$. NaCl-$SS_{(40)}$ are control plants subjected to the neighbouring airborne cue of NaCl-S plants, whilst NaCl-$S_{(40)}$ are step 1 smelling plants irrigated with water for another 20 days. Plants that were not previously exposed to volatiles and irrigated with water were used as controls, namely $C_{(40)}$. Step 3: after 20 days, NaCl-SS plants were treated with 60 mM NaCl (NaCl-SS+$NaCl_{(60)}$), $C_{(40)}$ were treated with 60 mM NaCl ($C+NaCl_{(60)}$) and plants that were not previously exposed to volatiles and irrigated with water were used as controls, namely $C_{(60)}$.

Oven UN30, Schwabach, Germany) at 105 °C until the constant weight was reached.

Leaf Na^+ content determination was obtained according to Ceccanti et al. (2022) using an Agilent ICP-EOS 5900 (Agilent Technologies, Santa Clara, USA). Data are expressed as mg Na^+ per g dry weight (DW).

Leaf Cl^- concentration was determined according to Ceccanti et al. (2021) using an ion-exchange chromatograph (Dionex DX120, Dionex Corporation, Sunnyvale, CA, USA). Data are expressed as mg Cl^- per g DW.

2.4. Gas exchange analyses

Gas exchange measurements were carried out using a portable infrared gas analyzer (LI-6400, Li-Cor, Lincoln, NE, USA) on randomly selected fully expanded leaves between 10:00 a.m. and 1:00 pm. under ambient light conditions of 600 μmol m^{-2} s^{-1}. The CO_2 concentration in the leaf chamber was set to 400 μmol mol^{-1} using a CO_2 mixer, and the flow rate was mantained 500 μmol s^{-1}. After reaching a steady state, net photosynthetic rate (P_n), stomatal conductance (g_s) and intercellular CO_2 concentration (C_i) were recorded. The apparent carboxylation efficiency was determined by calculating the ratio of P_n to C_i.

2.5. Total chlorophyll and carotenoid content determination

Chlorophylls and carotenoids were extracted from the leaf fresh material according to Papadakis et al. (2018). Total chlorophyll (Chl_{TOT}) and carotenoid (Car_{TOT}) concentrations were determined according to Landi et al. (2020). Data are expressed as mg Chl_{TOT} or Car_{TOT} per g DW.

2.6. Lipid peroxidation level assay

The level of lipid peroxidation was assessed by determining the concentration of malondialdehyde (MDA), the final product of lipid peroxidation, using the method outlined by Hodges et al. (1999). Briefly, 100 mg of fresh strawberry leaves from each step of the experiment were homogenized with 6 mL of an 80 % (v/v) ethanolic aqueous solution and centrifuged at maximum speed for 10 min. Subsequently, 1 mL of supernatant was combined with 1 mL of 0.5 % thiobarbituric acid dissolved in 20 % trichloroacetic acid solution (TCA; w/v), while another 1 mL of supernatant was mixed with 1 mL of 20 % TCA solution. Both mixtures were incubated at 95 °C for 30 min, allowed to cool, and then the absorbance of the resulting supernatant was measured at 532, 600, and 440 nm. MDA equivalents were calculated using the molar extinction coefficient(ε) of MDA, 157,000 M^{-1} $cm^{-}1$, and expressed as mmol MDA g^{-1} fresh weight (FW).

2.7. Metabolite extraction, sample derivatization and Gc–Ms analysis

Plant materials were obtained by powdering and freeze-drying fresh strawberry leaves in liquid nitrogen. A hundred mg of lyophilized leaves were used, for each sample and replication. Sample extraction was performed according to Landi et al. (2020). After the extraction, the upper polar phases (150 μL) for each sample and replicate were collected and dried in a vacuum concentrator at room temperature. Derivatization was performed according to Landi et al. (2020). For the GC–MS analysis, derivatized samples (110 μL per sample and treatment) were transferred into glass vials.

The derivatized extracts were injected into a MEGA 5-MS capillary column (30 *m* × 0.25 mm × 0.25 μm + 10 m of pre-column) using a gas chromatograph apparatus (GC Agilent series 7890A) equipped with a single quadrupole mass spectrometer (MSD 5975C inert XL Perf Turbo) using, for sample handling and injection, a combiPAL autosampler following Araniti et al. (2022) method and settings.

Baseline filtering and calibration, peak alignment, deconvolution, integration of the peak height and annotation were carried out using the open-source software MS-DIAL (Misra et al. 2020). For metabolite annotation and assignment of the EI-MS spectra, the metabolomics standards initiative (MSI) guidelines for the metabolite identification were followed (Sansone et al. 2007), using Level 2 [identification based on the spectral database (match factor > 80 %)] and Level 3 (putatively annotated compound class based on spectral similarity to known compounds of a chemical class as suggested). Falsely annotated metabolites were discarded.

2.8. VOCs analysis

For headspace-solid phase microextraction (SPME), Supelco SPME devices coated with divinylbenzene/carboxen/polydimethylsiloxane (DVB/CAR/PDMS, 50/30/30 μm) were used. Third terminal fresh leaves were collected from various parts of the plant, placed immediately into a 100-mL glass conical flask, letting them equilibrate for 20 min, and then exposed to the headspace for 10 min at room temperature. After sampling, the fiber was withdrawn into the needle and transferred to the injection port of the GC–MS system. GC–MS analyses were performed with a gas chromatograph (Agilent 7890B, Palo Alto, CA, USA) equipped with an HP-5 capillary column (30 *m* × 0.25 mm; 0.25 μm coating thickness) and a single quadrupole mass detector (Agilent 5977B, Palo Alto, CA, USA). The acquisition parameters were: i) full scan; ii) scan range: 30–300 *m/z*; iii) scan time 1.0 s. Injector, transfer line and oven temperatures were set according to Landi et al. (2020). Standard sample retention times and their linear retention indices relative to a series of *n*-hydrocarbons were used to identify constituents; furthermore, mass spectra were matched against a commercial (NIST 2014 and ADAMS)

and a home-made library of mass spectra built up from pure substances and mixtures of known compounds. Semiquantitative relative peak areas (%) comparisons were performed between the same chemicals in the different samples.

2.9. Statistical analysis

The normality of data was evaluated with the Shapiro-Wilk test, while homoscedasticity of data was assessed with Bartlett's test. All data were subjected to a one-way analysis of variance (ANOVA) with salt stress as the source of variation. Means were separated using Fisher's least significant difference (LSD) *post-hoc* test ($p \leq 0.05$). Statistical analyses were conducted with GraphPad software (GraphPad, La Jolla, CA, USA). Volatilome data were normalized and then classified through a Principal Component Analysis (PCA) using JMP Pro 16 (SAS Institute Inc., Cary, NC, USA).

Regarding the GC–MS analysis of the metabolic profile, a completely randomized design with three biological replications was adopted. Samples were divided into two groups (first group [$C_{(20)}$], [C+$NaCl_{(20)}$], [NaCl-$S_{(20)}$]; second group [$C_{(40)}$], [C+$NaCl_{(40)}$], [NaCl-$S_{(40)}$], [NaCl-S + $NaCl_{(40)}$], [NaCl-$SS_{(40)}$]) and separately analysed. Statistical analysis for the putative annotated metabolites of GC–MS data sets was performed on normalized intensities using MetaboAnalyst version 5.0 (Pang et al. 2021). Briefly, relative abundance values from the MS-DIAL outputs were normalized per the internal standard, square-root transformed, and Pareto scaled. Successively, univariate analysis (ANOVA using LSD test as *post-hoc* $p \leq 0.05$), multivariate analysis [unsupervised principal component analysis (PCA) and supervised PLS-DA or sPLS-DA] and machine learning analysis were used. The PLS-DA model was built using the first three latent variables, and the performance of the model was validated through the Leave-One-Out Cross-Validation (LOOCV) using Q_2 as a performance measure. If the built model was overfitting, the data were further analyzed through the sparse Partial Least Squares Discriminant Analysis (sPLS-DA)], which was built using two components (components 1 and 2), selecting the top 19 variables (metabolites) for both components and validated using LOOCV as validation method. The selection of components and features number was carried out according to Lê Cao et al. (2011), and the estimated classification error rates for GC–MS data set with respect to each sPLS-DA dimension are reported in the Suppl. S1 (excel sheet - sPLSDA-Loadings).

Finally, the machine learning analysis Random Forest was used to classify and select features. The classification was randomized using 500 trees and seven predictors.

3. Results

3.1. Plant biomass and dry matter percentage

Table 1 summarizes plant biomass and dry matter results in the three steps. In step 1, the salt treatment led to a reduction in leaf biomass in *C*+$NaCl_{(20)}$ plants compared to the control group (–32.1 %), whilst no significant differences were observed between $C_{(20)}$ and NaCl-$S_{(20)}$ and between NaCl-$S_{(20)}$ and *C*+$NaCl_{(20)}$. Consequently, the salt treatment induced an increase in dry matter in *C*+$NaCl_{(20)}$ plants, whereas both controls and receivers had similar values in dry matter percentage. In step 2, the salt treatment induced a reduction in plant biomass of *C*+$NaCl_{(40)}$ plants, whilst similar results in biomass were found in controls and receivers, but also in NaCl-$SS_{(40)}$ and NaCl-*S*+$NaCl_{(40)}$ plants. No significant differences in dry matter percentage were found between all theses in step 2. In step 3, a reduction in biomass was observed in NaCl-SS+$NaCl_{(60)}$ (–32.9 %) and *C*+$NaCl_{(60)}$ (–27.3 %) plants and an increase in dry matter was observed in *C*+$NaCl_{(60)}$ (+10.0 %) plants when compared with controls. No significant differences in dry matter percentage were found between $C_{(60)}$ and NaCl-SS+$NaCl_{(60)}$ plants and between the latter and C-$NaCl_{(60)}$ plants.

Table 1
Plant biomass and dry matter percentage. Leaf biomass production and dry weight percentage of strawberry (*Fragaria* × *ananassa* var. Elsanta) plants irrigated with water at 20 [$C_{(20)}$], 40 [$C_{(40)}$] or 60 [$C_{(60)}$] days of treatment, irrigated with 60 mM NaCl at 20 [C+$NaCl_{(20)}$], 40 [*C*+$NaCl_{(40)}$] or 60 [C+$NaCl_{(60)}$] days of treatment, irrigated with water and grown together with C+$NaCl_{(20)}$ plants [NaCl-$S_{(20)}$] or with C+$NaCl_{(40)}$ plants [NaCl-$S_{(40)}$], NaCl-S plants further irrigated with 60 mM NaCl for 20 days [NaCl-*S* + $NaCl_{(40)}$], $C_{(40)}$ plants irrigated with water and growth with NaCl-$S_{(40)}$ plants [NaCl-$SS_{(40)}$] and NaCl-SS plants irrigated with 60 mM NaCl [NaCl-SS+$NaCl_{(60)}$]. Data (means ± SD, $n = 3$) were subjected to one-way ANOVA and different letters are significantly different at $p \leq 0.05$ after LSD *post-hoc* test with different treatments as the only source of variability.

	Total biomass (g $plant^{-1}$)	Dry matter (%)
	Step 1	
$C_{(20)}$	25.49 ± 1.20^{a}	13.47 ± 0.88^{b}
C+$NaCl_{(20)}$	17.32 ± 0.90^{b}	19.09 ± 1.67^{a}
NaCl-$S_{(20)}$	22.01 ± 4.55^{ab}	12.97 ± 0.89^{b}
	Step 2	
$C_{(40)}$	26.74 ± 3.14^{a}	17.18 ± 1.52^{a}
C+$NaCl_{(40)}$	22.00 ± 1.60^{b}	19.26 ± 1.08^{a}
NaCl-$S_{(40)}$	30.43 ± 2.78^{a}	16.56 ± 1.62^{a}
NaCl-*S*+$NaCl_{(40)}$	27.11 ± 1.87^{a}	17.00 ± 1.65^{a}
NaCl-$SS_{(40)}$	30.73 ± 2.02^{a}	16.45 ± 0.66^{a}
	Step 3	
$C_{(60)}$	38.56 ± 0.29^{a}	17.59 ± 0.67^{b}
C+$NaCl_{(60)}$	28.04 ± 4.24^{b}	19.54 ± 0.38^{a}
NaCl-SS+$NaCl_{(60)}$	25.88 ± 5.58^{b}	18.60 ± 0.89^{ab}

3.2. Gas exchange analyses

In step 1, P_n values decreased in both C+$NaCl_{(20)}$ and NaCl-$S_{(20)}$ plants compared to controls (–27 and –9 %, respectively; Fig. 2a). A similar trend was also detected for g_s showing lower values in both C+$NaCl_{(20)}$ and NaCl-$S_{(20)}$ plants compared to controls (–29 and –8 %, respectively; Fig. 2b). No statistical differences were observed in C_i in step 1 (Fig. 2c). Similarly to P_n and g_s, also P_n/C_i recorded a significant decrease in C+$NaCl_{(20)}$ and NaCl-$S_{(20)}$ plants (–29 and –9 %, respectively; Fig. 2d). In step 2, P_n values significantly decreased only in C+$NaCl_{(40)}$ plants (–9 % than controls; Fig. 2e). No differences in g_s between controls and the other treatments were observed, even though the highest values were recorded for NaCl-$SS_{(40)}$ and NaCl-S+$NaCl_{(40)}$ (0.352 and 0.340 mol m^{-2} s^{-1}, respectively) and the lowest for C+$NaCl_{(40)}$ plants (0.307 mol m^{-2} s^{-1}; Fig. 2f). No statistical differences were observed in C_i in step 2 (Fig. 2 g). P_n/C_i values significantly decreased only in C+$NaCl_{(40)}$ plants (–9 % compared to the controls; Fig. 2h). In step 3, P_n and g_s values decreased at a similar extent in both C+$NaCl_{(60)}$ and NaCl-SS+$NaCl_{(60)}$ plants compared to controls (~12 %; Fig. 2i,j). No statistical differences were observed in C_i in step 3 (Fig. 2k). Lastly, P_n/C_i values decreased at a similar extent in both C+$NaCl_{(60)}$ and NaCl-SS+$NaCl_{(60)}$ plants compared to controls (~15 %; Fig. 2l).

3.3. Chl_{TOT} and Car_{TOT} content

Table 2 summarizes the leaf Chl_{TOT} and Car_{TOT} concentration results in the three steps. In step 1, a decrease in Chl_{TOT} was only observed in C+$NaCl_{(20)}$ plants (–19 % compared to $C_{(20)}$), whereas similar results were found between $C_{(20)}$ and NaCl-$S_{(20)}$. No differences in Car_{TOT} between the controls and the other treatments were observed. The highest Car_{TOT} values were recorded for NaCl-$S_{(20)}$ (3.83 mg g^{-1} DW), while the lowest for C+$NaCl_{(20)}$ plants (2.97 mg g^{-1} DW). In step 2, Chl_{TOT} contents significantly decreased only in C+$NaCl_{(40)}$ plants (–26 % compared to $C_{(40)}$). Car_{TOT} decreased significantly in NaCl-$SS_{(40)}$, NaCl-$S_{(40)}$ and C+$NaCl_{(40)}$ plants compared to controls (–7, –22 and –25 %, respectively). In step 3, the salt treatment reduced the Chl_{TOT} contents in both NaCl-SS+$NaCl_{(60)}$ and C+$NaCl_{(60)}$ plants compared to controls (~13 %). The Car_{TOT} content significantly decreased only in C+$NaCl_{(60)}$ plants

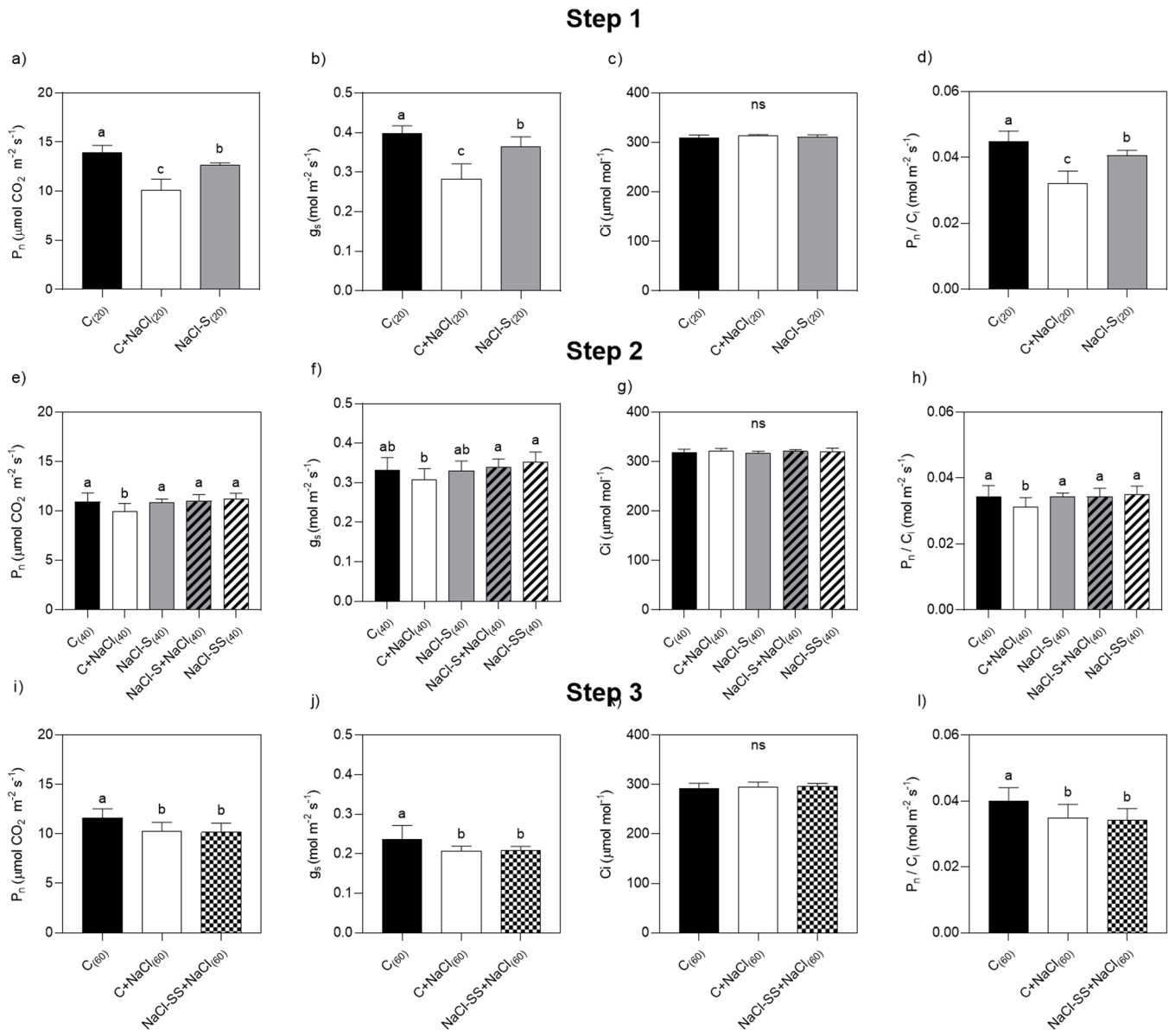

Fig. 2. Gas exchenge results. Gas exchange parameters of strawberry (*Fragaria* × *ananassa* var. Elsanta) plants irrigated with water at 20 [$C_{(20)}$], 40 [$C_{(40)}$] or 60 [$C_{(60)}$] days of treatment, irrigated with 60 mM NaCl at 20 [$C+NaCl_{(20)}$], 40 [$C+NaCl_{(40)}$] or 60 [$C+NaCl_{(60)}$] days of treatment, irrigated with water and grown together with $C+NaCl_{(20)}$ plants [NaCl-$S_{(20)}$] or with $C+NaCl_{(40)}$ plants [NaCl-$S_{(40)}$], NaCl-S plants further irrigated with 60 mM NaCl for 20 days [NaCl-*S* + $NaCl_{(40)}$], $C_{(40)}$ plants irrigated with water and growth with NaCl-$S_{(40)}$ plants [NaCl-$SS_{(40)}$] and NaCl-SS plants irrigated with 60 mM NaCl [NaCl-SS+$NaCl_{(60)}$]. Net photosynthetic rate (P_n; a, e, i), stomatal conductance (g_s; b, f, j), intercellular CO_2 concentration (C_i; c, g, k), and apparent carboxylation efficiency (P_n/C_i; d, h, l) of step 1, 2 and 3 respectively. Data (means ± SD, $n = 8$) were subjected to one-way ANOVA, and bars with different letters are significantly different at $p \leq 0.05$ after LSD *post-hoc* test with different treatments as the only source of variability.

compared to controls (–14 %).

3.4. Leaf Na^+ and Cl^- assimilation

Table 3 summarizes the leaf Na^+ and Cl^- concentration results in the three steps. In step 1, the salt treatment induced an increase in Na^+ and Cl^- assimilation when compared to $C_{(20)}$ and NaCl-$S_{(20)}$ (+87.2 % and +86.0 %, respectively), whilst no significant differences in Na^+ and Cl^- assimilation were found between controls and receivers. In step 2, the highest Na^+ and Cl^- assimilation was found in $C+NaCl_{(40)}$ (15.21 mg g^{-1} DW) followed by receivers subjected to salt treatment (14.09 mg g^{-1} DW). In step 3, both NaCl-SS+$NaCl_{(60)}$ and $C+NaCl_{(60)}$ plants showed an increase in $Na^+$and Cl^- assimilation when compared with controls (+69.1 % and +70.4 %, respectively).

3.5. Lipid peroxidation level

In step 1, an increase in leaf lipid peroxidation level was induced by salt treatment ($C+NaCl_{(20)}$) when compared to $C_{(20)}$ and NaCl-$S_{(20)}$, whereas similar results of MDA content were found in controls and receivers (Fig. 3a). In step 2, the level of lipid peroxidation increased in NaCl-*S*+$NaCl_{(40)}$ plants as well as in emitters ($C+NaCl_{(40)}$) when compared to controls (+49.7 % and +53.2 %, respectively) and receivers. No significant differences were found between NaCl-$S_{(40)}$ and NaCl-$SS_{(40)}$ plants, nor between the latter treatment and the controls. The lowest lipid peroxidation level was found in controls (81.5 mmol g^{-1} FW; Fig. 3b). In step 3, higher values of lipid peroxidation were found in $C+NaCl_{(60)}$ and NaCl-SS+$NaCl_{(60)}$ when compared to $C_{(60)}$ (Fig. 3c).

Table 2
Total chlorophyll and carotenoid content. Total leaf chlorophyll (Chl_{TOT}) and carotenoid (Car_{TOT}) concentrations of strawberry (*Fragaria* × *ananassa* var. Elsanta) plants irrigated with water at 20 [$C_{(20)}$], 40 [$C_{(40)}$] or 60 [$C_{(60)}$] days of treatment, irrigated with 60 mM NaCl at 20 [C+$NaCl_{(20)}$], 40 [*C*+$NaCl_{(40)}$] or 60 [C+$NaCl_{(60)}$] days of treatment, irrigated with water and grown together with C+$NaCl_{(20)}$ plants [NaCl-$S_{(20)}$] or with C+$NaCl_{(40)}$ plants [NaCl-$S_{(40)}$], NaCl-S plants further irrigated with 60 mM NaCl for 20 days [NaCl-*S* + $NaCl_{(40)}$], $C_{(40)}$ plants irrigated with water and growth with NaCl-$S_{(40)}$ plants [NaCl-$SS_{(40)}$] and NaCl-SS plants irrigated with 60 mM NaCl [NaCl-SS+$NaCl_{(60)}$]. Data (means ± SD, $n = 4$) were subjected to one-way ANOVA, and different letters are significantly different at $p \leq 0.05$ after LSD *post-hoc* test with different treatments as the only source of variability.

	Chl_{TOT} (mg g^{-1} DW)	Car_{TOT} (mg g^{-1} DW)
	Step 1	
$C_{(20)}$	23.37 ± 0.88[a]	3.38 ± 0.32[ab]
C+$NaCl_{(20)}$	18.91 ± 2.53[b]	2.97 ± 0.31[b]
NaCl-$S_{(20)}$	23.68 ± 1.68[a]	3.83 ± 0.26[a]
	Step 2	
$C_{(40)}$	21.64 ± 1.30[a]	3.29 ± 0.30[a]
C+$NaCl_{(40)}$	16.11 ± 1.23[b]	2.48 ± 0.21[c]
NaCl-$S_{(40)}$	21.63 ± 2.75[a]	2.55 ± 0.36[c]
NaCl-S+$NaCl_{(40)}$	21.29 ± 1.05[a]	3.20 ± 0.17[ab]
NaCl-$SS_{(40)}$	20.86 ± 1.24[a]	3.06 ± 0.34[b]
	Step 3	
$C_{(60)}$	16.19 ± 1.09[a]	2.71 ± 0.12[a]
C+$NaCl_{(60)}$	14.19 ± 0.66[b]	2.35 ± 0.27[b]
NaCl-SS+$NaCl_{(60)}$	13.95 ± 0.29[b]	2.49 ± 0.04[ab]

Table 3
Na^+ and Cl^- accumulation. Cl^- and Na^+ accumulation in strawberry (*Fragaria* × *ananassa* var. Elsanta) plants irrigated with water at 20 [$C_{(20)}$], 40 [$C_{(40)}$] or 60 [$C_{(60)}$] days of treatment, irrigated with 60 mM NaCl at 20 [C+$NaCl_{(20)}$], 40 [C+$NaCl_{(40)}$] or 60 [C+$NaCl_{(60)}$] days of treatment, irrigated with water and grown together with C+$NaCl_{(20)}$ plants [NaCl-$S_{(20)}$] or with C+$NaCl_{(40)}$ plants [NaCl-$S_{(40)}$], NaCl-S plants further irrigated with 60 mM NaCl for 20 days [NaCl-S + $NaCl_{(40)}$], $C_{(40)}$ plants irrigated with water and growth with NaCl-$S_{(40)}$ plants [NaCl-$SS_{(40)}$] and NaCl-SS plants irrigated with 60 mM NaCl [NaCl-SS+$NaCl_{(60)}$]. Data (means ± SD, $n = 3$) were subjected to one-way ANOVA, and different letters are significantly different at $p \leq 0.05$ after LSD *post-hoc* test with different treatments as the only source of variability.

	Na^+ (mg g^{-1} DW)	Cl^- (mg g^{-1} DW)
	Step 1	
$C_{(20)}$	0.11 ± 0.02[b]	3.57 ± 0.13[b]
C+$NaCl_{(20)}$	7.08 ± 0.98[a]	27.81 ± 2.31[a]
NaCl-$S_{(20)}$	0.12 ± 0.00[b]	3.90 ± 0.43[b]
	Step 2	
$C_{(40)}$	0.13 ± 0.03[c]	3.64 ± 0.29[c]
C+$NaCl_{(40)}$	2.08 ± 0.04[a]	15.21 ± 0.51[a]
NaCl-$S_{(40)}$	0.34 ± 0.07[b]	4.06 ± 0.48[c]
NaCl-S+$NaCl_{(40)}$	1.59 ± 0.08[b]	14.09 ± 1.04[b]
NaCl-$SS_{(40)}$	0.16 ± 0.03[c]	4.43 ± 0.32[c]
	Step 3	
$C_{(60)}$	0.20 ± 0.02[b]	3.57 ± 0.09[b]
C+$NaCl_{(60)}$	1.56 ± 0.01[a]	12.04 ± 2.26[a]
NaCl-SS+$NaCl_{(60)}$	1.66 ± 0.12[a]	11.55 ± 0.90[a]

3.6. Metabolomic profile

The GC–MS analysis was conducted on plants from steps 1 and 2, identifying both grouped and individual metabolites that allowed sample discrimination. A total of 123 metabolites were putatively annotated and quantified across all samples, alongside 2342 unknown EI-MS features that were shared among the samples (Suppl. Table S1).

The PCA Score Plot, based on the first (PC1) and second (PC2) component, showed good discrimination between the sample groups, blanks, and QC, demonstrating the robustness of the model. In addition, the selected components effectively distinguished between treatments without any outliers, suggesting that our metabolomic analysis was consistent and accurately captured the metabolic changes in the plants throughout the experiment (Data not shown).

In step 1, the univariate ANOVA analysis highlighted that the treatments significantly altered 45 out of 123 annotated metabolites. Among them, 19 are sugars, 17 are organic acids, and 3 are amino acids (Suppl.Table S1).

The unsupervised PCA, built by *virtue* of the first two components (PCs), accounted for 65.6 % of the total variance. PC1 described 37.1 % while PC2 28.5 % of the total variance (Fig. 4a). In particular, the PCA analysis revealed a weak overlapping between C_{20} and NaCl-$S_{(20)}$ treatments and a clear separation from C+$NaCl_{(20)}$ samples.

The PCA loading plots evaluation, which highlighted the main contributors to sample separation, pointed out that the PC1 was mainly dominated by 1,3-dihydroxyacetone, phosphoric acid, quinic acid, citric acid, and L-proline, among others (Suppl. Table S1). In contrast, D-arabitol, citric acid, fructose, mannose, psicose, 1,3-dihydroxyacetone, and phosphoric acid mainly dominated PC2 (Suppl. Table S1).

A PLS-DA model was applied to maximise the covariance between metabolite levels and treatments; however, it failed to pass the cross-validation test, indicating potential overfitting (Suppl.Table S1). Consequently, the data were reanalysed using the supervised sPLS-DA method (Fig. 4b). In Fig. 4c,d, the weight of the loading vectors for each dimension of the sPLS-DA analysis, included in the variable selection, are plotted. Only features with a non-zero weight were considered and included in the variable selection (Fig. 4c,d).

The results pointed out an improvement in group separation, and the sPLS-DA-derived loading revealed that inosine, orotic acid, nicotinic acid, glycyl proline, 2-deoxy-D-glucose, among others, were the main metabolites influencing the PC1. In contrast, asparagine, psicose, fructose, isocitric acid, sorbose and ornithine influenced PC2 (Fig. 4c,d). Finally, the machine learning Random Forest analysis revealed β-ketoadipic acid, ribose, glutamic acid, 2-deoxy-D-glucose, and β-mannosylglycerate, among others, as the metabolites with the highest mean decrease accuracy (features ranked by their contributions to classification accuracy) for the three sample groups (Fig. 4e).

In step 2, the previously described shared metabolites (the same number of metabolites identified in step 1 and step 2) were analysed through one-way ANOVA using LSD as a *post-hoc* test ($p \leq 0.05$). The results showed that 74 out of 123 putatively annotated metabolites were significantly altered among treatments. In particular, 25 organic acids, 24 sugars, 10 amino acids, and among these, some are plant specialized metabolites (Suppl. Table S2).

The unsupervised PCA, built by *virtue* of the first two components (PCs), accounted for 64.2 % (42.9 % for PC1, 14.3 % for PC2) of the total variance. The score plot clearly separated all examined groups (Fig. 5a). However, the NaCl-*S*+$NaCl_{(40)}$ treatment was the more distant in the PCA space, whereas the other four treatments (although perfectly separated) were closer, clustering together (Fig. 5a). The loading plots of the main two components used for sample grouping pointed out that L-aspartic acid, shikimic acid, pinitol, DL-threo-β-methylaspartic acid, inositol, L-glutamic acid, fumaric acid, among others, were the main metabolites dominating the PC1, whereas PC2 was mainly dominated by L-ascorbic acid, citric acid, β-D-(+)-glucose, L-(-)-sorbose, D-arabitol, L-iditol, D-(-)-fructose (Suppl. Table S2).

The PLS-DA analysis, validated through cross-validation and permutation test with a number of permutations equal to 20 (Suppl. S2, excel sheet - PLS-DA_VIP_AND_Permutation), further confirmed the metabolic differences among all treatment groups. The VIP score highlighted that sugars (arabitol, iditol, fructose, sorbose, etc.) and organic acids (DL-threo-β-methylaspartic acid, succinic, fumaric and malic acid, among others) were the variables of importance in projection, mainly participating in groups separation (Fig. 5b,c). Finally, Random Forest analysis also highlighted that sorbose, ribose, arginine, tranexamic acid and fructose, among others, were the metabolites with the highest mean decrease accuracy (Fig. 5d).

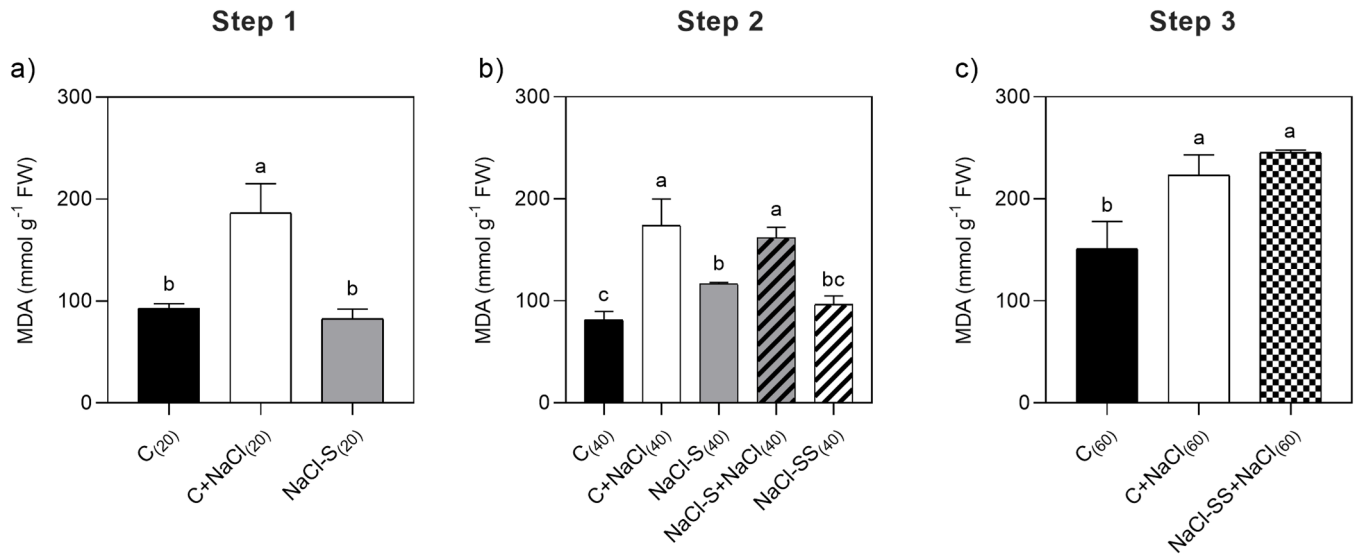

Fig. 3. Lipid peroxidation level. MDA production level of strawberry (*Fragaria* × *ananassa* var. Elsanta) plants irrigated with water at 20 [$C_{(20)}$], 40 [$C_{(40)}$] or 60 [$C_{(60)}$] days of treatment, irrigated with 60 mM NaCl at 20 [C+$NaCl_{(20)}$], 40 [C+$NaCl_{(40)}$] or 60 [C+$NaCl_{(60)}$] days of treatment, irrigated with water and grown together with C+$NaCl_{(20)}$ plants [NaCl-$S_{(20)}$] or with C+$NaCl_{(40)}$ plants [NaCl-$S_{(40)}$], NaCl-S plants further irrigated with 60 mM NaCl for 20 days [NaCl-*S* + $NaCl_{(40)}$], $C_{(40)}$ plants irrigated with water and growth with NaCl-$S_{(40)}$ plants [NaCl-$SS_{(40)}$] and NaCl-SS plants irrigated with 60 mM NaCl [NaCl-SS+$NaCl_{(60)}$] of step 1 (a), 2 (b) and 3 (c). Data (means ± SD, $n = 3$) were subjected to one-way ANOVA, and bars with different letters are significantly different at $p \leq 0.05$ after LSD *post-hoc* test with different treatments as the only source of variability.

3.7. VOCs profile

The GC–MS analysis carried out on VOCs was performed on plants from step 1 to step 2, allowing the identification of 68 metabolites belonging to the class of monoterpene hydrocarbons, oxygenated monoterpenes, sesquiterpene hydrocarbons, phenylpropanoids, apocarotenoids, non-terpene hydrocarbons, non-terpene aldehydes/ketones, non-terpene alcohols/ethers, non-terpene esters (Suppl. Table S3).

The multivariate treatment of HS-SPME analysis unveiled that the VOC fingerprint is altered by the salinity level imposed in the present experiment. Indeed, the unsupervised multivariate analysis carried out on the step 1 VOCs profiles and built on the first two components explained 73.5 % of the total variance, with PC1 describing 47.6 % and PC2 25.9 % (Fig. 6a). The analysis pointed out a clear separation between $C_{(20)}$, C+$NaCl_{(20)}$ and NaCl-$S_{(20)}$ plants. As reported by the loading plots, PC1 was mainly influenced by (*E,E*)-α-farnesene, germacrene D, α-humulene, cyclosativene, and decanal, whereas PC2 by cyclosativene, α-ylangene, limonene, methyl salicylate, (*E*)-hex-3-enyl-(*E*)-2-methylbut-2-enoate and (*E,E*)-α-farnesene, suggesting that those metabolites were significantly involved in samples separation (Suppl. Table S4). Fig. 6 clearly distinguishes the concentration trends of the metabolites under the three treatments, highlighting that some of them, especially those characterized by the higher VIP score (undecanal, cyclosativene, dodecanal, α-ylangene, among others) significantly increased in the treatment *C*+$NaCl_{(20)}$, reaching the highest concentrations in the treatment NaCl-$S_{(20)}$ (Fig. 6c). On the contrary, metabolites such as *n*-dodecane, 1-tetradecane, 2,4,6-trimethylacetophenone, 1-dodecane, and naphthalene strongly decreased their concentrations in C+$NaCl_{(20)}$ and NaCl-$S_{(20)}$ plants, when compared to controls (Fig. 6c).

Concerning step 2, the unsupervised PCA analysis (Fig. 7a), explained 65.6 % of the total variance, with PC1 describing 37.7 % and PC2 27.9 % of the total variance. Despite the perfect separation, NaCl-S+$NaCl_{(40)}$ clustered together with the groups C+$NaCl_{(40)}$ and NaCl-$S_{(40)}$. Instead, $C_{(40)}$ and NaCl-$SS_{(40)}$ partially overlapped on the PCA space. The loading plots pointed out that PC1 was dominated by nonanal, decanal, α-ylangene, cyclosativene, (*E*)-hex-3-enyl (*E*)-2-methylbut-2-enoate, δ-cadinene, (*E,E*)-α-farnesene, benzaldehyde, 1-hexyl acetate, whereas PC2 by β-caryophyllene, germacrene D, cyclosativene, α-ylangene, δ-cadinene, limonene, (*Z*)-3-hexenyl acetate, methyl salicylate (Suppl. Table S5). Again, the data were further examined using supervised PLS-DA (Fig. 7b), enhancing group separation and enabling the identification of key variables (VIP scores) driving it (Fig. 7c). The results, highlighting a mixed trend among the treatments, were reported on a false colour scale (Fig. 7c).

After multivariate analysis, the results were further analysed through univariate one-way ANOVA, which revealed that the treatments significantly altered 6 VOCs in step 1 (Suppl. Figure S1) and 16 in step 2 (Suppl. Figure S2). In particular, in step 1, salt stress decreased 1,8-cineole, α-muurolene, and (Z)-3-hexenyl acetate content when compared to control and increased (*E,E*)-α-farnesene and (*E*)-hex-3-enyl (*E*)-2-methylbut-2-enoate compared to controls. Receivers spurred 1,8-cineole and α-muurolene contents compared to $C_{(20)}$ and C+$NaCl_{(20)}$. NaCl-$S_{(20)}$ showed intermediate values for (*E*)-hex-3-enyl (*E*)-2-methylbut-2-enoate and (*Z*)-3-hexenyl acetate content when compared to $C_{(20)}$ and *C*+$NaCl_{(20)}$ metabolite content. Receivers did not significantly change (*E,E*)-α-farnesene and α-humulene content compared to controls, even though salt stress enhanced volatile content in the first case and decreased it in the latter (Suppl. Figure S1).

In step 2, salt stress significantly altered compound contents except for 2,4,6-trimethylacetophenone, β-caryophyllene, camphor, (*E*)-geranylacetone, and germacrene D, which remained unchanged compared to control. The receivers NaCl-$S_{(40)}$ revealed analogous content of 1-hexyl acetate, benzaldehyde, β-caryophyllene, decanal, and δ-cadinene compared to C+$NaCl_{(40)}$. NaCl-*S*+$NaCl_{(40)}$ significantly enhanced the content of 2,4,6-trimethylacetophenone, β-caryophyllene, and germacrene-D compared to C+$NaCl_{(40)}$. NaCl-$SS_{(40)}$ showed similar contents of 1-hexyl acetate, benzaldehyde, β-caryophyllene, decanal, and δ-cadinene compared to $C_{(40)}$, while revealed intermediate values than control and C+$NaCl_{(40)}$ plants for α-ylangene, cyclosativene, and (*E,E*)-α-farnesenene. NaCl-$SS_{(40)}$ significantly increased 2,4,6-trimethylacetophenone content compared to $C_{(40)}$ and C+$NaCl_{(40)}$. NaCl-$SS_{(40)}$ spurred decanal, methyl salicylate, and (*Z*)-3-hexenyl acetate but decreased 1-hexyl acetate, benzaldehyde, β-caryophyllene, δ-cadinene, (*E,E*)-α-farnesenene, and germacrene D content compared to NaCl-$S_{(40)}$ (Suppl. Figure S2).

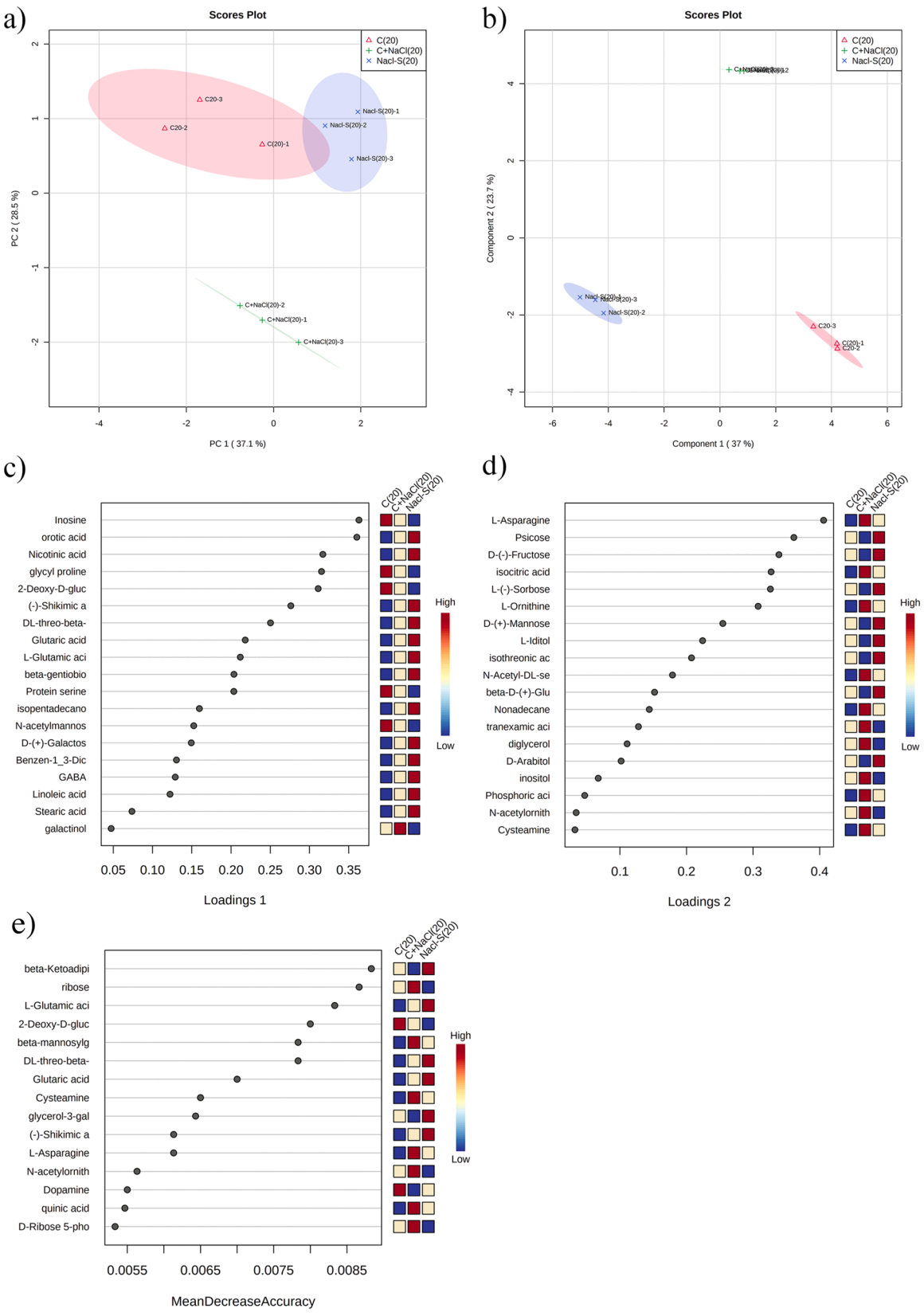

Fig. 4. Metabolomic profile (Step 1). Discrimination through principal component analysis (PCA) and partial least square discriminant analysis (PLS-DA) of the metabolite's patterns in strawberry (*Fragaria* × *ananassa* var. Elsanta) plants irrigated with water [$C_{(20)}$], with 60 mM NaCl [$C+NaCl_{(20)}$], or irrigated with water and grown together with $C+NaCl_{(20)}$ plants [$NaCl\text{-}S_{(20)}$] for 20 days (step 1). (a) PCA and (b) sPLS-DA plots allowed group discrimination by virtue of the first two components (PCs). sPLS-DA loading vectors for PC1 (c) and PC2 (d). (e) Random forest analysis displaying the mean decrease accuracies ($n = 3$).

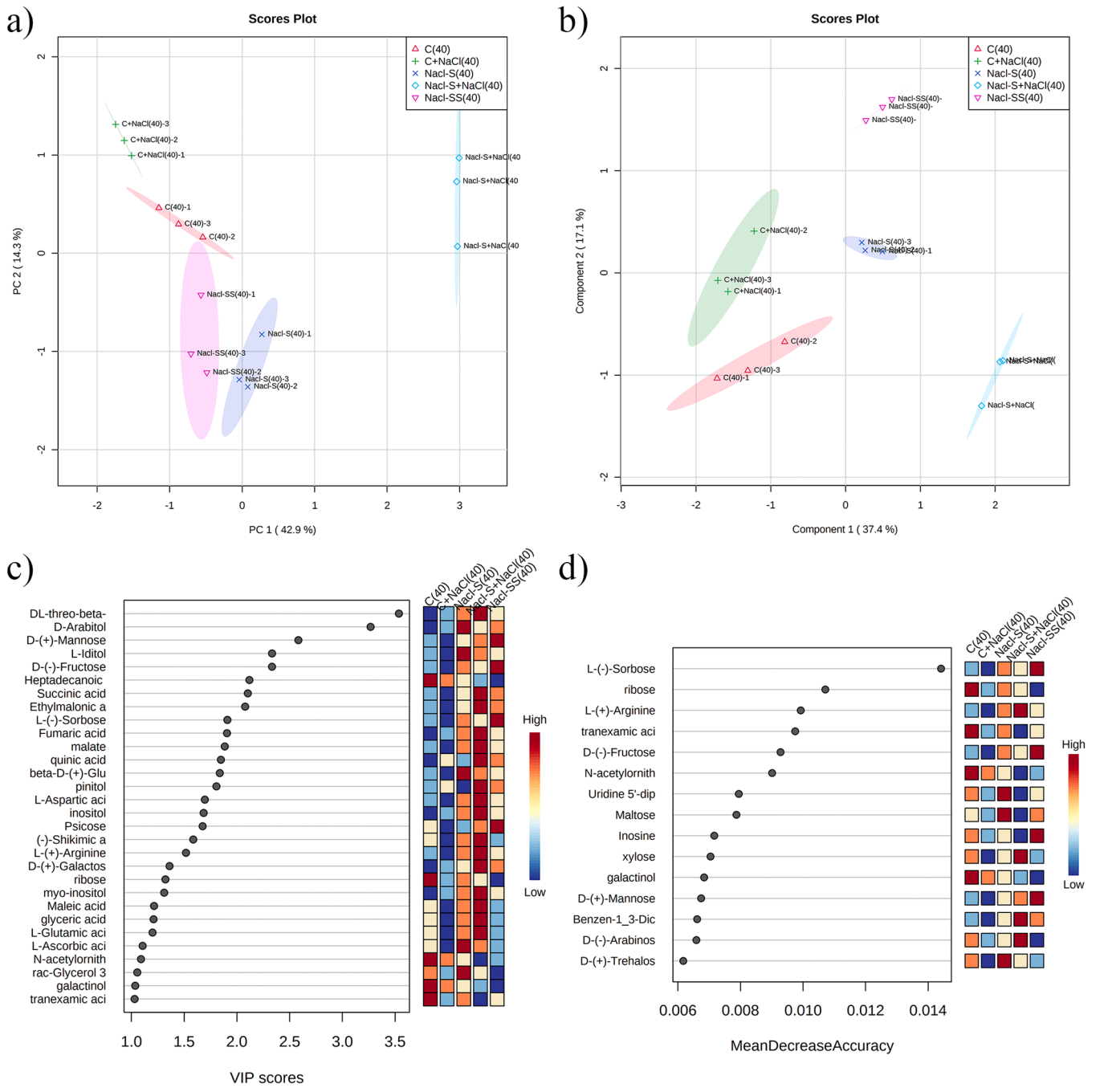

Fig. 5. Metabolomic profile (Step 2). Discrimination through principal component analysis (PCA) and partial least square discriminant analysis (PLS-DA) of the metabolites patterns in strawberry (*Fragaria* × *ananassa* var. Elsanta) plants irrigated with water [$C_{(40)}$], with 60 mM NaCl [C+$NaCl_{(40)}$], irrigated with water and grown together with C+$NaCl_{(40)}$ plants [NaCl-$S_{(40)}$], NaCl-S plants further irrigated with 60 mM NaCl [NaCl-S + $NaCl_{(40)}$], and $C_{(40)}$ plants irrigated with water and growth with NaCl-$S_{(40)}$ plants [NaCl-$SS_{(40)}$] for 20 days (step 2). (a) PCA and (b) PLS-DA showing score plots that allowed group discrimination by virtue of the first two principal components (PCs). (c) Variable importance of projection (VIP) features for the groups from PLS-DA analysis. (d) Random forest analysis displaying the mean decrease accuracies (n = 3).

4. Discussion

The current experiment aimed to provide a comprehensive understanding of the volatile profile and metabolic adaptations in strawberry plants when subjected to salt stress or when compelled to coexist with neighbouring salt-stressed plants. This investigation sought to determine whether the airborne signals can confer an ecological advantage to plants exposed to and "indirectly involved" in abiotic stress. Indeed, in the present scenario, VOC emissions and perception were the only viable ways for the inter-plant interaction since the direct physical contact and/or differences in growing environmental parameters (e.g., the influence on detecting a reduced ratio of red to far-red light reflected from neighbouring foliage or changes in relative humidity and plant gas exchange) were carefully considered and minimized.

4.1. Does (and how) salinity affect salt-stressed strawberry plants' metabolism and their volatilome?

Since global soil salinity issues are growing, there is an increasing need to develop new and environmentally friendly methods to induce

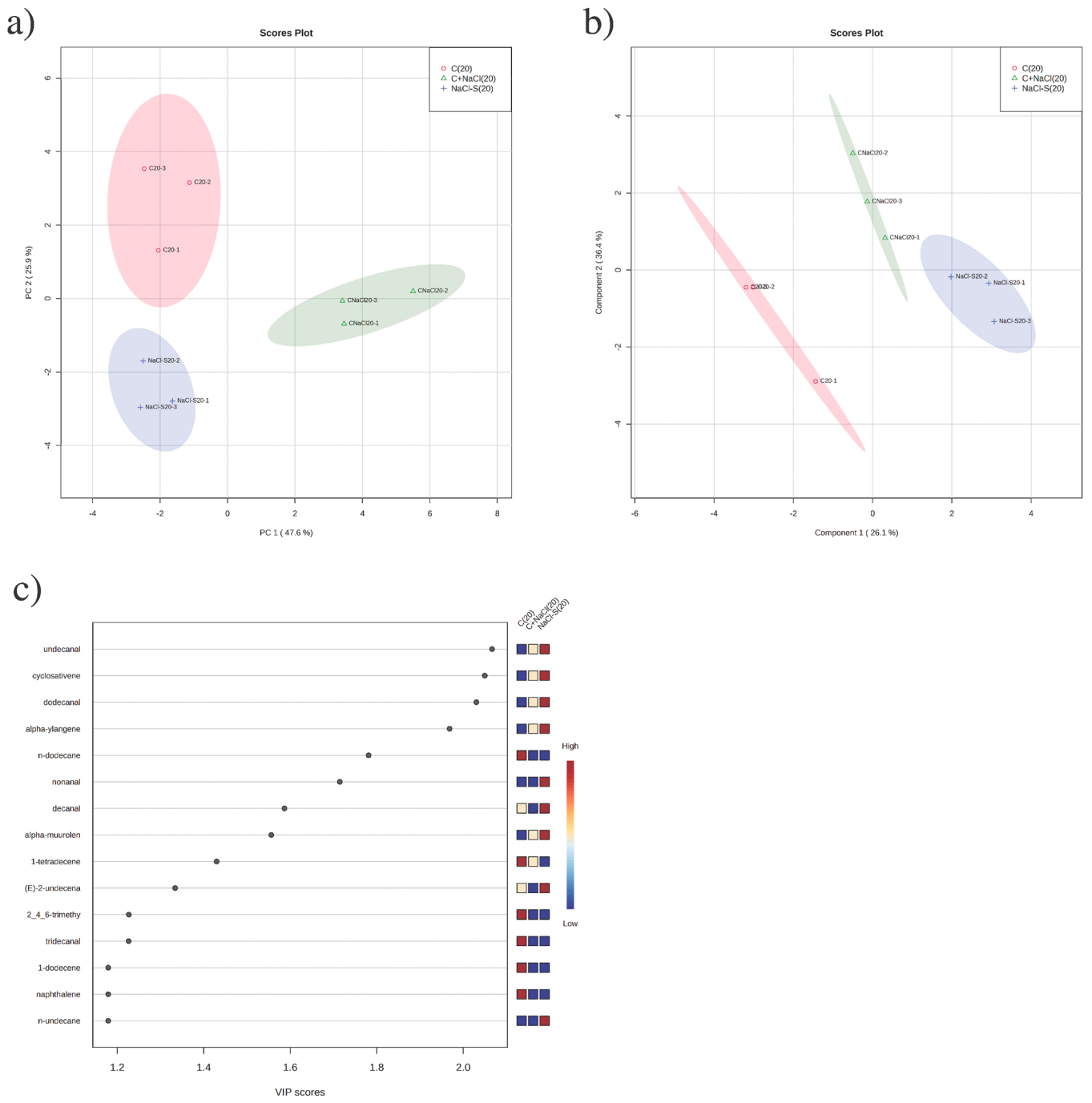

Fig. 6. VOC's profile (Step 1). Discrimination through principal component analysis (PCA) and supervised partial least squares discriminant analysis (PLS-DA) of the VOCs metabolites patterns in strawberry (*Fragaria* × *ananassa* var. Elsanta) plants irrigated with water [$C_{(20)}$], with 60 mM NaCl [C+$NaCl_{(20)}$], or irrigated with water and grown together with C+$NaCl_{(20)}$ plants [NaCl-$S_{(20)}$] for 20 days (step 1). (a) PCA, (b) sPLS-DA plots allowed group discrimination by virtue of the first two components (PCs), and (c) Variable Importance of Projection (VIP) features for the groups from PLS-DA analysis ($n = 3$).

salt stress tolerance in plants. Identification of airborne signals may represent a feasible approach for improving plant adaptation to such abiotic stresses. Soil salinity effects on plants have already been well-studied in scientific literature. Excessive salt concentration in the plant growing substrate induces root osmotic stress, preventing shoot and leaf water uptake from plant root apparatus (as reviewed by Chaves et al. 2009). These limitations lead to a decline in plant water potential and translocation and leaf cell turgor, stimulating stomatal closure and reducing cell growth (Ibrahimova et al. 2021). Moreover, $Na^+$and Cl^- can also be excessively translocated to leaf tissue, causing the onset of leaf cell osmotic imbalances (Tezara 2003; Sanchez-Blanco et al. 2004; Mereu et al. 2011; Calzone et al. 2020) and decreasing carbon assimilation efficiency due to an impaired stomatal conductance and to biochemical limitations (Sharkey 1990; Meyer and Genty 1998; Zahra et al. 2022). Not by chance all the C+$NaCl_{(20),(40),(60)}$ plants that increased their contents in Na^+ and Cl^-in leaves reduced P_n values paralleled by lower g_s values compared to $C_{(20),(40),(60)}$ plants with consequent decreased final biomass. At the same time, the steadiness of C_i values at lower g_s values than C plants can be explained by the increase in biochemical limitations, as indicated by the decline in apparent carboxylation efficiency (Chaves et al. 2009).

Salt stress generally also results in oxidative damage, causing

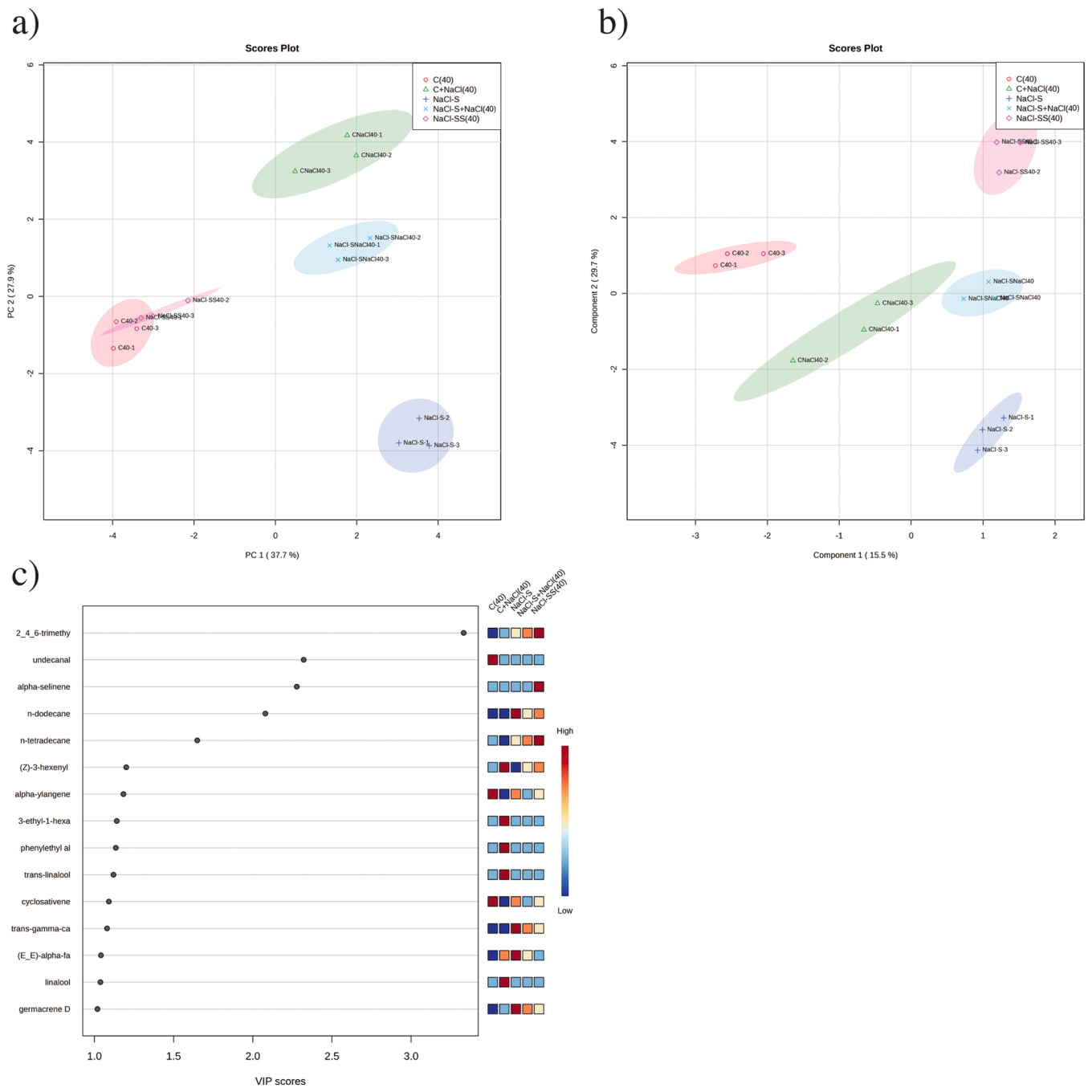

Fig. 7. VOC's profile (Step 2). Discrimination through principal component analysis (PCA) and supervised partial least squares discriminant analysis (PLS-DA) of the VOCs metabolites patterns in strawberry (*Fragaria* × *ananassa* var. Elsanta) plants irrigated with water [$C_{(40)}$], with 60 mM NaCl [$C+NaCl_{(40)}$], irrigated with water and grown together with $C+NaCl_{(40)}$ plants [$NaCl\text{-}S_{(40)}$], NaCl-S plants further irrigated with 60 mM NaCl [NaCl-*S* + $NaCl_{(40)}$], and $C_{(40)}$ plants irrigated with water and growth with $NaCl\text{-}S_{(40)}$ plants [$NaCl\text{-}SS_{(40)}$] for 20 days (step 2). (a) PCA, (b) PLS-DA showing score plots that allowed group discrimination by virtue of the first two principal components (PCs), (c) Variable importance of projection (VIP) features for the groups from PLS-DA analysis ($n = 3$).

chlorophyll degradation and affecting several cellular components and, in particular, altering chloroplast ultrastructures, chloroplast membrane transporters and causing membrane lipid peroxidation (Gupta and Huang 2014; Taïbi et al. 2016; Zahra et al. 2022). In the present experiment, a decrease in Chl_{TOT} content was found in C+NaCl plants belonging to all three steps. This alteration was already reported by several authors who assert that oxidative stress may inhibit chlorophyll synthesis and enhance its degradation by the enzyme chlorophyllase, thus resulting in a decreased chlorophyll level under salt stress conditions (Rao and Rao 1981; Santos 2004; Zhu et al. 2019). Moreover, in the present experiment, when compared with controls, a higher MDA content was found in salt-stressed plants in all three steps. These results agree with the findings of other authors who analyzed strawberry plants (Gulen et al. 2006; Garriga et al. 2015). For example, Gulen et al. (2006) noted an increase in peroxidase isozyme activities in leaves from three strawberry cultivars exposed to 8.5, 17.0 and 34.0 mM NaCl for 30 days. Garriga et al. (2015) observed a higher MDA level in leaves from Camarosa and Bau strawberry cultivars subjected to 30 or 60 mM NaCl for 4 weeks.

Moreover, the excessive absorption of toxic ions (i.e., Na^+ and Cl^-) in salt-stressed plants observed in the present experiment can induce an early ionic imbalance in leaves with a consequent alteration of primary

and secondary metabolism (Munns et al. 2006; Mudgal et al. 2010). Therefore, metabolic adjustments occur to activate plant responses against salt stress. Among primary metabolites, osmotic adjustments were ensured by amino acids, carbohydrates, and polyols increase, while ionic imbalances might be compensated by a depletion of organic acids (López-Bucio et al. 2000; Sanchez et al. 2007; Chaves et al. 2009). The results of the present experiment showed an increase in amino acids and polyamine (e.g., γ-aminobutyric acid, glutamate and ornithine), organic and inorganic acids (e.g., shikimic acid, isocitric acid, phosphoric acid), and pyridine carboxylic acids (e.g., nicotinic acid) in C+NaCl$_{(20)}$ compared to the control plant of step 1, in line with what was found by other authors (Yang and Guo 2018; Arif et al. 2020; Landi et al. 2020). However, the content of some organic acids, such as galactonic acid, gluconic acid, isothreonic acid, and mannoic acid decreased in C+NaCl$_{(20)}$ when compared with C$_{(20)}$, thereby being involved in the compensation of ionic Na^+ and Cl^- imbalance (as reviewed by Sanchez et al. 2007). This aspect was evident also from the results of step 2, where the content of most organic acids (e.g., aconitic acid, benzene-1,3 dicarboxylic acid, ethylmalonic acid, malate, mesonic acid, toluic acid and succinic acid) reported a decrease in C+NaCl$_{(40)}$ when compared with C$_{(40)}$, confirming the role of the organic acids in the compensation of ionic imbalance.

The production of osmoprotectants and osmolytes is generally considered a defense mechanism plants adopt to regulate cellular homeostasis in case of salt or drought stress (Singh et al. 2015). In particular, sugars such as glucose, fructose, and trehalose protect membranes and proteins. In contrast, sugar alcohols such as inositol enhance plant tolerance to salinity, by regulating osmotic balance and promoting, among other strategies, Na^+ sequestration in the vacuole (review by Singh et al. 2015). Despite what was expected, in the present experiment, some sugars and polyalcohols found in strawberry leaves, which should carry out an osmoprotectant role, decreased in both the steps (e.g., inositol and fructose in step 1 and glucose, fructose, and trehalose for step 2). The decrease in organic acid and sugar content noted in step 2 was reversed in NaCl-S+NaCl$_{(40)}$ plants, suggesting a priming effect of salt-stressed plants on neighbouring plants, responses that will be analyzed in depth in the next paragraph of the present work.

In addition to these plant responses, another intriguing area of research focuses on the release of VOCs by plants under salt stress. Plants emit a remarkable number of VOCs, such as terpenoids, aldehydes, and alcohols, with several functions, including defense against herbivores, signaling to neighbour plants, and mediating responses to environmental stressors (McCormick et al. 2012; Baldwin et al. 2002; Landi 2020). Water deficit conditions induced by salt stress can stimulate the production and release of certain VOCs, which might play roles in signaling and defense (Landi 2020). In our experiment, in both steps 1 and 2, the emission of some specific stress-related VOCs belonging to monoterpene hydrocarbons (e.g., (*E*)-β-ocimene), oxygenated monoterpenes (e.g., linalool), sesquiterpene hydrocarbons (e.g., (*Z, E*)-α-farnesene), and non-terpene alcohols/ethers (e.g., phenylethyl alcohol) was observed in salt-stressed plants. Among all the compounds emitted by C+NaCl$_{(20)}$ and C+NaCl$_{(40)}$ plants, 1,8-cineole is highly sensitive to salinity stress and variations in the content of this metabolite in essential oils have frequently been described in the literature (Talebi et al. 2018; Valifard et al. 2019; Vafadar Shoshtari 2017; Ben Ayed et al. 2022). In fact, an increase in the content of 1,8-cineole was observed in the essential oils from salt-stressed *Ocimum basilicum* and *Salvia mirzayanii* plants (Talebi et al. 2018; Valifard et al. 2019), whilst a decrease in the content of this VOC was noted in the essential oils produced by leaves from *Myrtus communis* and *Laurus nobilis* salt-stressed plants (Vafadar Shoshtari 2017; Ben Ayed et al. 2022). Thus, the variation in 1, 8-cineole content that occurred in the emitters (C+NaCl) of the present study confirmed the involvement of this volatile molecule in salt-stressed plant response. Moreover, variations in well-known green leaf volatiles (GLVs) such as (*Z*)-3-hexenyl acetate and sesquiterpenes such as β-caryophyllene were also recorded. The involvement of these metabolites could be pivotal, as their mechanisms of action, among other volatiles, are somewhat explored. It was demonstrated that once perceived by neighbouring plants, these compounds could initiate plasma membrane potential depolarization (Zebelo et al. 2012) and cytosolic Ca^{2+} concentration responses (Aratani et al. 2023) as early events in plant-plant communication. The rise of Ca^{2+} cytosolic content combined with changes in cytosolic pH triggers various cellular functions in neighbouring plants, including signal transduction pathways involved in plant defense mechanism against salt stress (Kader and Lindberg 2010). These responses may affect physiological and biochemical features in emitter plants, which will be addressed in the next paragraph. However, the discussion of VOC results exhibits some critical points. For example, the alteration of VOC fingerprint and VOC relative abundance might also be dependent on the plant age (e.g., the progression of plant age was responsible for the emission of different VOCs such as camphor not detected in younger plants; Holopainen and Gershenzon 2010) and thus, results from steps 1 and 2 could not be compared with each other, but differences in treatments could only be discussed within steps. Moreover, to complicate the picture, the emission of other VOCs is constrained in salt-stressed plants independently (e.g., β-caryophyllene) or dependently (such as α-muurolene) on the plant age (Landi et al. 2020). As a result, establishing consistent cause-and-effect relationships driven by one or a few volatiles is challenging (Landi et al. 2020).

4.2. *Can salt-stressed strawberry plants (VOCs emitter) prime neighbouring plants (VOCs receivers) to have faster and more efficient defense responses when exposed to salt stress?*

Despite very little is known about the mechanism operating behind the transmission of a volatile signal due to abiotic stressors (Landi 2020), VOCs plant priming has already been observed and demonstrated by some authors in different species (Lee and Seo 2014; Caparrotta et al. 2018; Landi et al. 2020). The present results are the first to demonstrate the VOC priming effects induced by salt stress on strawberry plants.

Step 1 receiver plants, NaCl-S$_{(20)}$, showed reduced P_n compared to control plants due to a decreased g_s, even though no stress was applied to this treatment. Similar responses were recorded in *Vicia faba* leaves exposed to neighbouring salt-stressed plants (Caparrotta et al. 2018), whilst any differences in biomass or g_s were observed in leaves of *Pisum sativum, Vitis vinifera,* and *Ocimum basilicum* receiver plants, and in receiver in vitro culture of *Arabidopsis thaliana* in experiments testing different abiotic stresses (Falik et al. 2011; Lee and Seo 2014; Landi et al. 2020; Midzi et al. 2023), thus suggesting that the responses are species-specific and stress-dose-dependent. Despite the P_n decrease observed in NaCl-S$_{(20)}$, this alteration did not involve any variation in total biomass, water content, leaf pigment concentration and lipid peroxidation level when compared to controls in step 1. This suggests that, although some messages were perceived from VOCs, they did not entail the typical growth alteration, oxidative stress induction or chlorophyll degradation induced by biochemical limitations of real salt stress.

Conversely, in step 2, although the receiver plants were not physiologically altered after saline irrigation, in NaCl-S+NaCl$_{(40)}$ treatment, the priming effect jumped out clearly. Indeed, despite the plants being irrigated with the same saline solution, and this induced similar levels of lipid peroxidation compared to C+NaCl$_{(40)}$, Na^+ and Cl^- uptake was slightly but significantly reduced compared to C+NaCl$_{(40)}$. These results align with those of common chemical priming agents already tested in literature (e.g., brassinosteroids, glycine betaine, spermidine, α-tocopherol, or the combination of nitric oxide and sulfur), which reported that the application of such chemicals decreases Na^+ uptake by regulating the expression level of Na^+ transporter (Fatma et al. 2016; Zhang et al. 2016; Sofy et al. 2020; Su et al. 2020; Naqve et al. 2021). In salt-stressed *Nitraria tangutorum,* a reduced Na^+ accumulation was recorded after priming with gaseous methyl jasmonate compared to non-primed salt-stressed plants (Gao et al. 2021), while no effects of

methyl jasmonate occurred in *Crithmum maritimum* and *Citrus sinensis* (Labiad et al. 2021; Mahmoud et al. 2021). Contrary to our results, Landi et al. (2020) did not report any variation in Na^+ and Cl^- uptake in primed- or non-primed-salt-stressed basil plants, which resulted in a similar physiological alteration but different reproductive success between the two treatments. Thus, we can presume that in strawberry plants under the condition of the present experiment, the priming effect induced by VOCs may operate on limiting Na^+ uptake.

Moreover, neither the photosynthetic capacity nor Chl_{TOT} or Car_{TOT} contents were affected by salt stress in NaCl-S+$NaCl_{(40)}$ in contrast to what has been observed by Caparrotta et al. (2018) and Landi et al. (2020), who reported variably decreased photosynthetic parameter values and negative alteration on maximal PSII photochemical efficiency compared to control plants. The partial lack of alteration found in the present experiment resulted in unchanged total plant biomass in receivers compared to control plants, evidencing the increased salt-stress tolerance of the primed plants (i.e., NaCl-S+$NaCl_{(40)}$).

Regarding primary metabolites, the leaves analyzed from NaCl-$S_{(20)}$ showed an increase in the content of sugars such as glucose, gentibiose, arabinose, fructose, galactose, lyxose, mannose, and sorbose when compared with $C_{(20)}$ in step 1. This result suggests that, although salt-stressed plants (C-$NaCl_{(20)}$) underwent oxidative stress induced by saline conditions, foregoing the production of osmolytes and osmoprotectants, neighbouring receiver plants (NaCl-$S_{(20)}$) grown near salt-stressed plants increased the production of osmoprotectants such as glucose and fructose as a priming defense mechanism to regulate cell homeostasis against imminent abiotic stress as the salt stress but also as a carbon sink in plants subjected to salt stress (Singh et al. 2015; Landi et al. 2020). Moreover, the pattern of some organic acids and amino acids was similar to that found in salt-stressed plants and different by $C_{(20)}$. For example, benzene-1,3-dicarboxylic acid, hydroxybutyric acid, methyl-aspartic acid, γ-aminobutyric acid, glutaric acid, nicotinic acid, phosphoric acid, and shikimic acid increased in NaCl-$S_{(20)}$ when compared to $C_{(20)}$, as observed for the C-$NaCl_{(20)}$ plants. Others, such as galactonic acid, gluconic acid, and mannoic acid decreased in receivers when compared to control, exactly as noted in emitters. These results highlight and confirm the priming effect of salt-stressed plants on receiver plants. The priming effect also led to differences in the primary metabolism in NaCl-S+$NaCl_{(40)}$ treatment, which separated the most in the multivariate analysis compared to all the other treatments, showing increased content in amino acids (e.g., homoserine, glutamine, asparagine, arginine), organic acids (e.g., β-hydroxybutyric acid, aconitic acid, ethylmalonic acid, fumaric acid, glyceric acid, aspartic acid), sugars *in sensu latu* (including polyalcohols; e.g., lactose, glucose, gentibiose, arabinose, fructose, mannose, inositol, and myoinositol) compared to C+$NaCl_{(40)}$. These results agree with the findings reported by Landi et al. (2020), who observed an increase in sugars, including polyalcohols, in receiver basil plants exposed to salt stress when compared to their controls. The authors asserted that, similarly to salt-stressed plants, the incorporation of organic compounds such as sugars and amino acids can be utilized as osmoprotectants and carbon sinks also by receivers once subjected to salt stress (Landi et al. 2020). Results suggested that the response in NaCl-S+$NaCl_{(40)}$ plants resulted greater extended when compared with C+$NaCl_{(40)}$ since the priming effect in the first plants induced a more efficient response in primary metabolites (e.g., synthesis of osmoprotectants such as inositol and myoinositol) than in the second plants. Those metabolites are known for their role as stabilizers of several macromolecules, as well as cellular structures, photosynthetic complexes and specific enzymes (reviewed by Mehta and Vyas, 2023) thus, they may be behind the preserved photosynthetic capacity of NaCl-*S*+$NaCl_{(40)}$

How VOCs enhance salt stress tolerance by altering metabolic pathways still needs to be unveiled. Loreto and D'Auria (2022) hypothesize three different mechanisms of VOC perception. The first one involved plant possession of a VOC-sensing system mediated by receptors [e.g., the use of Odorant Binding Protein (OBP)-like protein receptors in case of methyl jasmonate, methyl ester of salicylic acid or a TOPLESS binding protein for β-caryophyllene). A second hypothesis considers that plants do not need OBP-Olfactory Receptors (ORs) systems to perceive VOCs. The last theory consists of a more direct way of sensing which does not require protein transporters and receptors but instead involves physical and chemical changes in cell membranes or scavenges of ROS.

In step 2, the VOCs blend emitted by the two salt-treated groups (C+$NaCl_{(40)}$ and NaCl-S+$NaCl_{(40)}$) was nearly identical, except for 2,4,6-trimethylacetophenone, β-caryophyllene, camphor, and germacrene D. Among these molecules, it was found that camphor and germacrene D were newly synthesized after saline treatment in *Salvia officinalis* and *Citrus aurantium*, respectively (Kulak et al. 2020; Lamine et al. 2020). Notably, β-caryophyllene plays as an allelochemical component in plant signaling networks, inducing stress tolerance through the upregulation of jasmonic acid- and salicylic acid-signaling pathways (Frank et al. 2021). Its perception in tobacco is attributed to a transcriptional co-repressor, a TOPLESS-like protein, initiating the expression of stress response genes (Nagashima et al. 2019). Moreover, the exogenous application of another GLV, (*Z*)-3-hexeny-1-yl acetate, has been reported to induce salinity stress tolerance in peanut plants, both by affecting roots and shoots and by reducing damages occurring at the photosystem level as well as the ROS content in peanut leaves (Tian et al. 2019). These results validate the hypothesis that VOCs (GLVs and others) emitted by stressed plants can prime neighbouring conspecific individuals, which, in turn, can induce more efficient defense responses (such as reducing ion uptake, preserving growth and physiological functions) when exposed to salt stress.

4.3. Are unstressed receivers able to propagate the message to neighbouring strawberry plants?

To the best of our knowledge, only Falik et al. (2011) have explored the possibility that receiver plants can transmit any signals received from stressed individuals to non-stressed neighbouring plants. Authors reported that further propagation of a drought stress signal among non-stressed *Pisum sativum* plants was impossible via shoot volatile emission but only through root exudates (Falik et al. 2011). Given the lack of awareness about the possibility of interactions from unstressed receivers to neighbouring plants, the present work represents an attempt to improve the knowledge of plant-to-plant signalling propagation by evaluating different plant species and abiotic stress.

Despite the variation observed in NaCl-$S_{(40)}$ in step 2, in which several metabolites were altered similarly to salt-stressed plants, NaCl-$SS_{(40)}$ partially overlapped control plants. Once stress was applied in step 3, those plants developed typical salt stress symptoms, namely reduced biomass, photosynthesis and Chl_{TOT} content and increased Na^+ and Cl^- leaf assimilation and lipid peroxidation levels, exactly as C-$NaCl_{(60)}$. Our results support Falik et al. (2011) observations as unstressed receivers' strawberry plants of the present experiment could not prime neighbours through the propagation of a salt stress alarm message to induce effective defense responses. All these pieces of evidence suggest that the possible VOC emissions from NaCl-$S_{(40)}$ may not be sufficient to propagate the message or to prime neighbouring plants or even that the spreading of a message through VOCs is not possible without a real stress. These doubts prompt the question of whether plants actually participate in signalling to warn neighbouring plants of the same species or whether the course of natural evolution has limited plants to merely decoding nearby volatile signals to trigger defensive mechanisms.

5. Conclusion

The present work offers new evidence about the propagation of volatile messages emitted by salt-stressed and unstressed strawberry plants and about the physiological and biochemical effect induced in neighbour conspecific plants which perceive these signals somewhat.

Results built up evidence of a relevant VOC emission shift from stressed and unstressed plants and identified some interaction-related and salt stress-related metabolites emitted and synthesized after the salt stress. Secondly, this work confirms that neighbouring strawberry plants can perceive and transduce those volatile signals, achieving a direct advantage against salt stress. Receiver plants, having altered their primary metabolite patterns to regulate cell homeostasis against imminent abiotic stress, once underwent the same stressful conditions, were able to reduce harmful effects and to preserve some growing and physiological characteristics, thus demonstrating the priming condition promoted by exogenous VOCs. Furthermore, the novelty of this research lies in evidence that receiver strawberry plants cannot propagate the salt-stress signal via volatile emission to their neighbouring conspecific plants. Thus, although the molecular mechanism of plant-plant interactions is still to be deciphered, this work delineates both the potentialities and the limits under which these interactions occur. Since the present research fulfils in answering the above questions, new issues urgently require an answer. i) What are the volatile metabolites which take part in signal transduction? It results in utmost importance to decipher those signals identifying the key metabolites involved in the delivery of the priming message. ii) What are the mechanisms of perception and transduction of such volatile signals in receiver plants? It is essential to generate a transcriptomic dataset of receivers, depicting a list of candidate genes potentially involved in the sensing of those VOCs. iii) If receivers cannot propagate the signal to conspecific neighbours, may they bequeath genetically or epigenetically this chemical information or the priming induction to their next generation? Evaluating a possible transgenerational stress memory in primed plants may have a crucial role both in the understanding of plant ecological behaviour and at the same time on the development of new agricultural practices.A call to action is needed to further explore this topic, given the possible direct application of specific volatiles in crops to tackle the challenges of environmental stress.

CRediT authorship contribution statement

Costanza Ceccanti: Formal analysis, Data curation. **Giulia Lauria:** Writing – original draft, Formal analysis, Data curation, Conceptualization. **Fabrizio Araniti:** Writing – review & editing, Investigation, Formal analysis, Data curation. **Ermes Lo Piccolo:** Writing – review & editing, Formal analysis, Data curation, Conceptualization. **Ylenia Pieracci:** Formal analysis, Data curation. **Guido Flamini:** Writing – review & editing, Formal analysis, Data curation. **Lucia Guidi:** Writing – review & editing, Investigation. **Marco Landi:** Writing – review & editing, Writing – original draft, Funding acquisition, Data curation, Conceptualization.

Declaration of competing interest

The authors declare that they have no known competing financial interests or personal relationships that could have appeared to influence the work reported in this paper.

Supplementary materials

Supplementary material associated with this article can be found, in the online version, at doi:10.1016/j.stress.2025.100855.

Data availability

The authors confirm that the data supporting the findings of this study are available within the article.

References

Araniti, F., Prinsi, B., Espen, L., 2022. The delay of *Raphanus raphanistrum* subsp. *sativus* (L.) domin seed germination induced by coumarin is mediated by a lower ability to sustain the energetic metabolism. Plants 11, 843. https://doi.org/10.3390/plants11070843.

Aratani, Y., Uemura, T., Hagihara, T., Matsui, K., Toyota, M., 2023. Green leaf volatile sensory calcium transduction in *Arabidopsis*. Nat. Commun. 14 (1), 6236. https://doi.org/10.1038/s41467-023-41589-9.

Arif, Y., Singh, P., Siddiqui, H., Bajguz, A., Hayat, S., 2020. Salinity induced physiological and biochemical changes in plants: an omic approach towards salt stress tolerance. Plant Physiol. Biochem. 156, 64–77. https://doi.org/10.1016/j.plaphy.2020.08.042.

Backster, C., 2003. In: Backster, C. (Ed.), Primary Perception: Biocommunication with Plants, Living Foods, and Human Cells. White Rose Millennium Press, CA.

Baldwin, I.T., Schultz, J.C., 1983. Rapid changes in tree leaf chemistry induced by damage: evidence for communication between plants. Science (1979) 221 (4607), 277–279. https://doi.org/10.1126/science.221.4607.277.

Baldwin, I.T., Kessler, A., Halitschke, R., 2002. Volatile signaling in plant–plant–herbivore interactions: what is real? Curr. Opin. Plant Biol. 5 (4), 351–354. https://doi.org/10.1016/S1369-5266(02)00263-7.

Baluška, F., 2009. In: Baluška, F. (Ed.), Plant-Environment Interactions: From Sensory Plant Biology to Active Plant Behavior. Springer-Verlag Berlin and Heidelberg GmbH & Co, Berlin, Germany.

Ben Ayed, A., Zanin, G., Aissa, E., Haouala, F., 2022. Volatile oil components of laurel (*Laurus nobilis* L.) leaves obtained from plants cultivated under salinity stress conditions. Horticulturae 8 (5), 442. https://doi.org/10.3390/horticulturae8050442.

Bibbiani, S., Colzi, I., Taiti, C., Guidi Nissim, W., Papini, A., Mancuso, S., Gonnelli, C., 2018. Smelling the metal: volatile organic compound emission under Zn excess in the mint *Tetradenia riparia*. Plant Sci. 271, 1–8. https://doi.org/10.1016/j.plantsci.2018.03.006.

Brosset, A., Blande, J.D., 2022. Volatile-mediated plant–plant interactions: volatile organic compounds as modulators of receiver plant defence, growth, and reproduction. J. Exp. Bot. 73 (2), 511–528. https://doi.org/10.1093/jxb/erab487.

Calzone, A., Cotrozzi, L., Pellegrini, E., Guidi, L., Lorenzini, G., Nali, C., 2020. Differential response strategies of pomegranate cultivars lead to similar tolerance to increasing salt concentrations. Sci. Hortic. 271, 109441. https://doi.org/10.1016/j.scienta.2020.109441.

Camacho-Coronel, X., Molina-Torres, J., Heil, M., 2020. Sequestration of exogenous volatiles by plant cuticular waxes as a mechanism of passive associational resistance: a proof of concept. Front. Plant Sci. 11, 121. https://doi.org/10.3389/fpls.2020.00121.

Caparrotta, S., Boni, S., Taiti, C., Palm, E., Mancuso, S., Pandolfi, C., 2018. Induction of priming by salt stress in neighboring plants. Environ. Exp. Bot. 147, 261–270. https://doi.org/10.1016/j.envexpbot.2017.12.017.

Ceccanti, C., Brizzi, A., Landi, M., Incrocci, L., Pardossi, A., Guidi, L., 2021. Evaluation of major minerals and trace elements in wild and domesticated edible herbs traditionally used in the Mediterranean area. Biol. Trace Elem. Res. 199, 3553–3561. https://doi.org/10.1007/s12011-020-02467-3.

Ceccanti, C., Lauria, G., Lo Piccolo, E., Guidi, L., Pezzarossa, B., Rosellini, I., Cardelli, R., Becagli, M., Landi, M., 2022. Assessment of leaf photosynthetic performances and bioaccumulation of trace metals by lettuce leaves and strawberry fruits amended with sewage sludge: which possible re-use in agriculture? Sci. Hortic. 295, 110884. https://doi.org/10.1016/j.scienta.2022.110884.

Chaves, M.M., Flexas, J., Pinheiro, C., 2009. Photosynthesis under drought and salt stress: regulation mechanisms from whole plant to cell. Ann. Bot. 103 (4), 551–560. https://doi.org/10.1093/aob/mcn125.

Ciriello, M., Cirillo, V., Formisano, L., De Pascale, S., Romano, R., Fusco, G.M., Nicastro, R., Carillo, P., Kyriacou, M.C., Soteriou, G.A., Rouphael, Y., 2023. Salt-induced stress impacts the phytochemical composition and aromatic profile of three types of basil in a genotype-dependent mode. Plants 12, 2167. https://doi.org/10.3390/plants12112167.

Engelberth, J., Engelberth, M., 2019. The costs of green leaf volatile induced-defense priming: temporal diversity in growth responses to mechanical wounding and insect herbivory. Plants 8, 23. https://doi.org/10.3390/plants8010023.

Falik, O., Mordoch, Y., Quansah, L., Fait, A., Novoplansky, A., 2011. Rumor has it…: relay communication of stress cues in plants. PLoS. One 6 (11), e23625. https://doi.org/10.1371/journal.pone.0023625.

Fatma, M., Masood, A., Per, T.S., Khan, N.A., 2016. Nitric oxide alleviates salt stress inhibited photosynthetic performance by interacting with sulfur assimilation in mustard. Front. Plant Sci. 7, 521. https://doi.org/10.3389/fpls.2016.00521.

Frank, L., Wenig, M., Ghirardo, A., van der Krol, A., Vlot, A.C., Schnitzler, J.P., Rosenkranz, M., 2021. Isoprene and β-caryophyllene confer plant resistance via different plant internal signalling pathways. Plant Cell Environ. 44 (4), 1151–1164. https://doi.org/10.1111/pce.14010.

Frost, C.J., Mescher, M.C., Carlson, J.E., De Moraes, C.M., 2008. Plant defense priming against herbivores: getting ready for a different battle. Plant Physiol. 146, 818–824. https://doi.org/10.1104/pp.107.113027.

Gao, Z., Gao, S., Li, P., Zhang, Y., Ma, B., Wang, Y., 2021. Exogenous methyl jasmonate promotes salt stress-induced growth inhibition and prioritizes defense response of *Nitraria tangutorum* Bobr. Physiol. Plant 172 (1), 162–175. https://doi.org/10.1111/ppl.13314.

Garriga, M., Muñoz, C.A., Caligari, P.D., Retamales, J.B., 2015. Effect of salt stress on genotypes of commercial (*Fragaria* × *ananassa*) and Chilean strawberry

(*F. chiloensis*). Sci. Hortic. 195, 37–47. https://doi.org/10.1016/j.scienta.2015.08.036.
Gulen, H., Turhan, E., Eris, A., 2006. Changes in peroxidase activities and soluble proteins in strawberry varieties under salt stress. Acta Physiol. Plant 28, 109–116. https://doi.org/10.1007/s11738-006-0037-7.
Gupta, B., Huang, B., 2014. Mechanism of salinity tolerance in plants: physiological, biochemical, and molecular characterization. Int. J. Genomics. 2014 (1), 701596. https://doi.org/10.1155/2014/701596.
Heil, M., Karban, R., 2010. Explaining evolution of plant communication by airborne signals. Trends. Ecol. Evol. 25, 137–144. https://doi.org/10.1016/j.tree.2009.09.010.
Himanen, S.J., Blande, J.D., Klemola, T., Pulkkinen, J., Heijari, J., Holopainen, J.K., 2010. Birch (*Betula* spp.) leaves adsorb and re-release volatiles specific to neighbouring plants – a mechanism for associational herbivore resistance? New. Phytol. 186, 722–732. https://doi.org/10.1111/j.1469-8137.2010.03220.x.
Hodges, D.M., DeLong, J.M., Forney, C.F., Prange, R.K., 1999. Improving the thiobarbituric acid-reactive-substances assay for estimating lipid peroxidation in plant tissues containing anthocyanin and other interfering compounds. Planta 207, 604–611. https://doi.org/10.1007/s004250050524.
Holopainen, J.K., Gershenzon, J., 2010. Multiple stress factors and the emission of plant VOCs. Trends. Plant Sci. 15, 176–184. https://doi.org/10.1016/j.tplants.2010.01.006.
İbrahimova, U., Kumari, P., Yadav, S., Rastogi, A., Antala, M., Suleymanova, Z., Zivcak, M., Tahjib-Ul-Arif, M., Hussain, S., Abdelhamid, M., Hajihashemi, S., Yang, X., Brestic, M., 2021. Progress in understanding salt stress response in plants using biotechnological tools. J. Biotechnol. 329, 180–191. https://doi.org/10.1016/j.jbiotec.2021.02.007.
Kader, M.A., Lindberg, S., 2010. Cytosolic calcium and pH signaling in plants under salinity stress. Plant Signal. Behav. 5 (3), 233–238. https://doi.org/10.4161/psb.5.3.10740.
Karban, R., 2015. Plant Sensing and communication. in Plant Sensing and Communication. University of Chicago Press. https://doi.org/10.7208/chicago/9780226264844.001.0001.
Kulak, M., Gul, F., Sekeroglu, N., 2020. Changes in growth parameter and essential oil composition of sage (*Salvia officinalis* L.) leaves in response to various salt stresses. Ind. Crops. Prod. 145, 112078. https://doi.org/10.1016/j.indcrop.2019.112078.
Labiad, M.H., Giménez, A., Varol, H., Tüzel, Y., Egea-Gilabert, C., Fernández, J.A., Martínez-Ballesta, M.D.C., 2021. Effect of exogenously applied methyl jasmonate on yield and quality of salt-stressed hydroponically grown sea fennel (*Crithmum maritimum* L.). Agronomy 11 (6), 1083. https://doi.org/10.3390/agronomy11061083.
Lamine, M., Gargouri, M., Mliki, A., 2020. Identification of the NaCl-responsive metabolites in citrus roots: a lipidomic and volatomic signature. Plant Signal. Behav. 15 (8), 1777376. https://doi.org/10.1080/15592324.2020.1777376.
Landi, M., Araniti, F., Flamini, G., Lo Piccolo, E., Trivellini, A., Abenavoli, M.R., Guidi, L., 2020. Help is in the air": volatiles from salt-stressed plants increase the reproductive success of receivers under salinity. Planta 251, 48. https://doi.org/10.1007/s00425-020-03344-y.
Landi, M., 2020. Airborne signals and abiotic factors: the neglected side of the plant communication. Commun. Integr. Biol. 13 (1), 67–73. https://doi.org/10.1080/19420889.2020.1767482.
Lauria, G., Lo Piccolo, E., Davini, A., Ruffini Castiglione, M., Pieracci, Y., Flamini, G., Martens, S., Angeli, A., Ceccanti, C., Guidi, L., Pellegrini, E., Incrocci, L., Landi, M., 2023. Modulation of VOC fingerprint and alteration of physiological responses after supplemental LED light in green-and red-leafed sweet basil (*Ocimum basilicum* L.). Sci. Hortic. 315, 111970. https://doi.org/10.1016/j.scienta.2023.111970.
Lê Cao, K.A., Boitard, S., Besse, P., 2011. Sparse PLS discriminant analysis: biologically relevant feature selection and graphical displays for multiclass problems. BMC. Bioinformatics. 12, 253. https://doi.org/10.1186/1471-2105-12-253.
Lee, K., Seo, P.J., 2014. Airborne signals from salt-stressed *Arabidopsis* plants trigger salinity tolerance in neighboring plants. Plant Signal. Behav. 9, e28392. https://doi.org/10.4161/psb.28392.
Li, T., Blande, J.D., 2015. Associational susceptibility in broccoli: mediated by plant volatiles, impeded by ozone. Glob. Chang. Biol. 21, 1993–2004. https://doi.org/10.1111/gcb.12835.
López-Bucio, J., Nieto-Jacobo, M.F., Ramırez-Rodrıguez, V., Herrera-Estrella, L., 2000. Organic acid metabolism in plants: from adaptive physiology to transgenic varieties for cultivation in extreme soils. Plant Sci. 160 (1), 1–13. https://doi.org/10.1016/S0168-9452(00)00347-2.
Loreto, F., Barta, C., Brilli, F., Nogues, I., 2006. On the induction of volatile organic compound emissions by plants as consequence of wounding or fluctuations of light and temperature. Plant Cell Environ. 29 (9), 1820–1828. https://doi.org/10.1111/j.1365-3040.2006.01561.x.
Loreto, F., D'Auria, S., 2022. How do plants sense volatiles sent by other plants? Trends. Plant Sci. 27 (1), 29–38. https://doi.org/10.1016/j.tplants.2021.08.009.
Lucas-Barbosa, D., van Loon, J.J., Gols, R., van Beek, T.A., Dicke, M., 2013. Reproductive escape: annual plant responds to butterfly eggs by accelerating seed production. Funct. Ecol. 27, 245–254. https://doi.org/10.1111/1365-2435.12004.
Mahmoud, L.M., Vincent, C.I., Grosser, J.W., Dutt, M., 2021. The response of salt-stressed Valencia sweet orange (*Citrus sinensis*) to salicylic acid and methyl jasmonate treatments. Plant Physiol. Rep. 26, 137–151. https://doi.org/10.1007/s40502-020-00563-z.
McCormick, A.C., Unsicker, S.B., Gershenzon, J., 2012. The specificity of herbivore-induced plant volatiles in attracting herbivore enemies. Trends. Plant Sci. 17 (5), 303–310. https://doi.org/10.1016/j.tplants.2012.03.012.
Mehta, D., Vyas, S., 2023. Comparative bio-accumulation of osmoprotectants in saline stress tolerating plants: a review. Plant Stress 9, 100177. https://doi.org/10.1016/j.stress.2023.100177.
Mereu, S., Gerosa, G., Marzuoli, R., Fusaro, L., Salvatori, E., Finco, A., Spano, D., Manes, F., 2011. Gas exchange and JIP-test parameters of two Mediterranean maquis species are affected by sea spray and ozone interaction. Environ. Exp. Bot. 73, 80–88. https://doi.org/10.1016/j.envexpbot.2011.02.004.
Meyer, S., Genty, B., 1998. Mapping intercellular CO2 mole fraction (*Ci*) in *Rosa rubiginosa* leaves fed with abscisic acid by using chlorophyll fluorescence imaging: significance of *Ci* estimated from leaf gas exchange. Plant Physiol. 116, 947–957. https://doi.org/10.1104/pp.116.3.947.
Midzi, J., Jeffery, D.W., Baumann, U., Capone, D.L., Rogiers, S.Y., Pagay, V., 2023. Evidence of bi-directional volatile-mediated communication between drought-stressed and well-watered grapevines (*Vitis vinifera* L.). Agronomy 13 (7), 1747. https://doi.org/10.3390/agronomy13071747.
Misra, B.B., Das, V., Landi, M., Abenavoli, M., Araniti, F., 2020. Short-term effects of the allelochemical umbelliferone on *Triticum durum* L. metabolism through GC–MS based untargeted metabolomics. Plant Sci., 110548 https://doi.org/10.1016/j.plantsci.2020.110548.
Mudgal, V., Madaan, N., Mudgal, A., 2010. Biochemical mechanisms of salt tolerance in plants: a review. Int. J. Bot. 6 (2), 136–143.
Munns, R., James, R.A., Läuchli, A., 2006. Approaches to increasing the salt tolerance of wheat and other cereals. J. Exp. Bot. 57, 1025–1043. https://doi.org/10.1093/jxb/erj100.
Nagashima, A., Higaki, T., Koeduka, T., Ishigami, K., Hosokawa, S., Watanabe, H., Matsui, K., Hasezawa, S., Touhara, K., 2019. Transcriptional regulators involved in responses to volatile organic compounds in plants. J. Biol. Chem. 294 (7), 2256–2266. https://doi.org/10.1074/jbc.RA118.005843.
Naqve, M., Wang, X., Shahbaz, M., Fiaz, S., Naqvi, W., Naseer, M., Mahmood, A., Ali, H., 2021. Foliar spray of alpha-tocopherol modulates antioxidant potential of okra fruit under salt stress. Plants 10 (7), 1382. https://doi.org/10.3390/plants10071382.
Pang, Z., Chong, J., Zhou, G., de Lima Morais, D.A., Chang, L., Barrette, M., Gauthier, C., P-É, Jacques, Li, S., Xia, J., 2021. MetaboAnalyst 5.0: narrowing the gap between raw spectra and functional insights. Nucleic. Acids. Res. 49, W388–W396. https://doi.org/10.1093/nar/gkab382.
Papadakis, I.E., Tsiantas, P.I., Tsaniklidis, G., Landi, M., Psychoyou, M., Fasseas, C., 2018. Changes in sugar metabolism associated to stem bark thickening partially assist young tissues of *Eriobotrya japonica* seedlings under boron stress. J. Plant Physiol. 231, 337–345. https://doi.org/10.1016/j.jplph.2018.10.012.
Rao, G.G., Rao, G.R., 1981. Pigment composition and chlorophyllase activity in pigeon pea (*Cajanus indicus* Spreng) and gingelley (*Sesamum indicum* L.) under NaCl salinity. Indian J. Exp. Biol.
Sánchez-Blanco, M.J., Rodríguez, P., Olmos, E., Morales, M.A., Torrecillas, A., 2004. Differences in the effects of simulated sea aerosol on water relations, salt content, and leaf ultrastructure of Rock-Rose plants. J. Environ. Qual. 33 (4), 1369–1375. https://doi.org/10.2134/jeq2004.1369.
Sanchez, D.H., Siahpoosh, M.R., Roessner, U., Udvardi, M., Kopka, J., 2007. Plant metabolomics reveals conserved and divergent metabolic responses to salinity. Physiol. Plant 132, 209–219. https://doi.org/10.1111/j.1399-3054.2007.00993.x.
Sansone, S.A., Fan, T., Goodacre, R., Griffin, J.L., Hardy, N.W., Kaddurah-Daouk, R., Kristal, B.S., Lindon, J., Mendes, P., Morrison, N., 2007. The metabolomics standards initiative. Nat. Biotechnol. 25, 846. https://doi.org/10.1007/s11306-007-0070-6.
Santos, C.V., 2004. Regulation of chlorophyll *b*iosynthesis and degradation by salt stress in sunflower leaves. Sci. Hortic. 103 (1), 93–99. https://doi.org/10.1016/j.scienta.2004.04.009.
Sharkey, T.D., 1990. Water stress effects on photosynthesis. Photosynthetica 24, 651–656.
Singh, M., Kumar, J., Singh, S., Singh, V.P., Prasad, S.M., 2015. Roles of osmoprotectants in improving salinity and drought tolerance in plants: a review. Rev. Environ. Sci. Biotechnol. 14, 407–426. https://doi.org/10.1007/s11157-015-9372-8.
Sofy, M.R., Elhawat, N., Alshaal, T., 2020. Glycine betaine counters salinity stress by maintaining high K^+/Na^+ ratio and antioxidant defense via limiting Na^+ uptake in common bean (*Phaseolus vulgaris* L.). Ecotoxicol. Environ. Saf. 200, 110732. https://doi.org/10.1016/j.ecoenv.2020.110732.
Su, Q., Zheng, X., Tian, Y., Wang, C., 2020. Exogenous brassinolide alleviates salt stress in *Malus hupehensis* Rehd. by regulating the transcription of NHX-type Na^+ ($K^{(+)}$)/H^+ antiporters. Front. Plant Sci. 11, 38. https://doi.org/10.3389/fpls.2020.00038.
Taïbi, K., Taïbi, F., Abderrahim, L.A., Ennajah, A., Belkhodja, M., Mulet, J.M., 2016. Effect of salt stress on growth, chlorophyll content, lipid peroxidation and antioxidant defence systems in *Phaseolus vulgaris* L. S. Afr. J. Bot. 105, 306–312. https://doi.org/10.1016/j.sajb.2016.03.011.
Talebi, M., Moghaddam, M., Pirbalouti, A.G., 2018. Methyl jasmonate effects on volatile oil compounds and antioxidant activity of leaf extract of two basil cultivars under salinity stress. Acta Physiol. Plant 40, 1–11. https://doi.org/10.1007/s11738-018-2611-1.
Tezara, W., Martínez, D., Rengifo, E., Herrera, A.N.A., 2003. Photosynthetic responses of the tropical spiny shrub *Lycium nodosum* (Solanaceae) to drought, soil salinity and saline spray. Ann. Bot. 92 (6), 757–765. https://doi.org/10.1093/aob/mcg199.
Tian, S., Guo, R., Zou, X., Zhang, X., Yu, X., Zhan, Y., Ci, D., Wang, M., Wang, Y., Si, T., 2019. Priming with the green leaf volatile (Z)-3-hexeny-1-yl acetate enhances salinity stress tolerance in peanut (*Arachis hypogaea* L.) seedlings. Front. Plant Sci. 10, 785. https://doi.org/10.3389/fpls.2019.00785.
Vafadar Shoshtari, Z., Rahimmalek, M., Sabzalian, M.R., Hosseini, H., 2017. Essential oil and bioactive compounds variation in myrtle (*Myrtus communis* L.) as affected by seasonal variation and salt stress. Chem. Biodivers. 14 (4), e1600365. https://doi.org/10.1002/cbdv.201600365.

Valifard, M., Mohsenzadeh, S., Kholdebarin, B., Rowshan, V., Niazi, A., Moghadam, A., 2019. Effect of salt stress on terpenoid biosynthesis in *Salvia mirzayanii:* from gene to metabolite. J. Hortic. Sci. Biotechnol. 94 (3), 389–399. https://doi.org/10.1080/14620316.2018.1505443.

Yang, Y., Guo, Y., 2018. Elucidating the molecular mechanisms mediating plant salt-stress responses. New. Phytol. 217 (2), 523–539. https://doi.org/10.1111/nph.14920.

Yuan, J.S., Himanen, S.J., Holopainen, J.K., Chen, F., Jr, Stewart CN, 2009. Smelling global climate change: mitigation of function for plant volatile organic compounds. Trends. Ecol. Evol. 24 (6), 323–331. https://doi.org/10.1016/j.tree.2009.01.012.

Zahra, N., Al Hinai, M.S., Hafeez, M.B., Rehman, A., Wahid, A., Siddique, K.H., Farooq, M., 2022. Regulation of photosynthesis under salt stress and associated tolerance mechanisms. Plant Physiol. Biochem. 178, 55–69. https://doi.org/10.1016/j.plaphy.2022.03.003.

Zebelo, S.A., Matsui, K., Ozawa, R., Maffei, M.E., 2012. Plasma membrane potential depolarization and cytosolic calcium flux are early events involved in tomato (*Solanum lycopersicon*) plant-to-plant communication. Plant Sci. 196, 93–100. https://doi.org/10.1016/j.plantsci.2012.08.006.

Zhang, N., Shi, X., Guan, Z., Zhao, S., Zhang, F., Chen, S., Fang, W., Chen, F., 2016. Treatment with spermidine protects chrysanthemum seedlings against salinity stress damage. Plant Physiol. Biochem. 105, 260–270. https://doi.org/10.1016/j.plaphy.2016.05.002.

Zhu, Y.F., Wu, Y.X., Hu, Y., Jia, X.M., Zhao, T., Cheng, L., Wang, Y.X., 2019. Tolerance of two apple rootstocks to short-term salt stress: focus on chlorophyll degradation, photosynthesis, hormone and leaf ultrastructures. Acta Physiol. Plant 41, 1–14. https://doi.org/10.1007/s11738-019-2877-y.